JGR Atmospheres

RESEARCH ARTICLE
10.1029/2021JD035487

Observations Indicate That Clouds Amplify Mechanisms of Southern Ocean Heat Uptake

Ariel L. Morrison[1], Hansi A. Singh[1], and Philip J. Rasch[2]

[1]School of Earth and Ocean Sciences, University of Victoria, Victoria, BC, Canada, [2]Atmospheric Sciences and Global Change Division, Pacific Northwest National Laboratory, Richland, WA, USA

Key Points:

- Anomalously strong annual mean Southern Ocean heat uptake is mainly controlled by reduced ocean heat loss during winter
- Changes in clouds and their associated atmospheric states amplify ocean heat uptake by increasing downward longwave radiation at the surface
- More clouds are linked to a more stable atmosphere which increases ocean heat uptake by suppressing turbulent heat fluxes out of the surface

Supporting Information:

Supporting Information may be found in the online version of this article.

Correspondence to:

A. L. Morrison,
arielmorrison@uvic.ca

Citation:

Morrison, A. L., Singh, H. A., & Rasch, P. J. (2022). Observations indicate that clouds amplify mechanisms of Southern Ocean heat uptake. *Journal of Geophysical Research: Atmospheres*, *127*, e2021JD035487. https://doi.org/10.1029/2021JD035487

Received 29 JUN 2021
Accepted 27 JAN 2022

Abstract The Southern Ocean has absorbed most of the excess heat associated with anthropogenic greenhouse gas emissions. Since Southern Ocean observations are sparse in certain regions and seasons, much of our knowledge of ocean heat uptake is based on climate model simulations. However, climate models still inadequately represent some properties of Southern Ocean clouds, and they have not identified the mechanisms by which clouds may affect Southern Ocean heat uptake (SOHU). Here, we use the ERA5 and JRA-55 reanalyses to assess the influence of clouds and other atmospheric processes on SOHU from 1979 to 2020. We find that years with the highest SOHU between 45° and 65°S are dominated by ocean heat uptake anomalies during winter and spring, but not during summer or fall. Winter and spring cloud cover are up to 7% higher when SOHU is up to 5.5 W/m^2 higher than the climatological seasonal mean, with the largest increases in the South Pacific Ocean. Clouds also contain more liquid water. These changes in cloud properties increase downwelling longwave radiation, amplifying ocean heat uptake. Cloud changes are also concomitant with a more stable lower atmosphere, which suppresses turbulent heat fluxes out of the surface. Overall, we find that SOHU is likely not mediated by enhanced surface shortwave absorption over the observational time period. A better understanding of how atmospheric processes impact ocean heat uptake may help improve our understanding of ocean heat uptake mechanisms in the current generation of climate models.

1. Introduction

The Southern Ocean is a fundamental regulator of global climate due to its ability to absorb, store, and transport heat. Through meridional overturning circulation and the formation of deep Antarctic Bottom Water, the Southern Ocean has absorbed an estimated 93% of the excess heat associated with anthropogenic warming (Rhein et al., 2013). It is estimated that by absorbing this excess heat, the Southern Ocean has reduced the rate of atmospheric warming and therefore the rate of global warming (e.g., Gregory, 2000). Though heat enters the deep ocean in both the North Atlantic and the Southern Ocean (Shi et al., 2018), results from the 5th Coupled Model Intercomparison Project (CMIP5; Taylor et al., 2012) show that the Southern Ocean is responsible for roughly 70% of global ocean heat uptake (Frölicher et al., 2015; Sallé, 2018). In an equilibrium state, the Southern Ocean would gain heat from the atmosphere during the spring and summer and lose heat to the atmosphere during fall and winter, with no net gain of heat to the ocean. Since the climate is not at equilibrium, however, the heat content of the Southern Hemisphere's oceans has increased by approximately $10*10^{22}$ J from the 1950s to 2000s (Gille, 2008). An increase in ocean heat content may manifest itself as an increase in heat absorption or a decrease in heat loss. As a result, the Southern Ocean has warmed over the past 50 years, though not uniformly: the upper 700 m have warmed by roughly 0.2°C per decade while regions of recently formed Antarctic Bottom Water have warmed by roughly 0.05°C per decade (Llovel & Terray, 2016; Purkey & Johnson, 2010; Rhein et al., 2013). Given the Southern Ocean's dominant role in global ocean heat uptake and mitigating warming from increased greenhouse gas emissions, understanding the interconnected mechanisms of Southern Ocean heat gain and loss is critical to reducing uncertainty in future climate projections.

Much research has focused on the oceanic mechanisms of heat uptake. Ocean heat gain and loss occur via different processes depending on the location, though most processes are related to ocean convection, upwelling, and northward heat transport. Due to strong westerly winds and Ekman divergence in the Southern Ocean, large-scale upwelling brings cold water to the surface, which acts as a sink for atmospheric heat (Gregory, 2000; Morrison et al., 2015). The continuous upwelling in this region maintains cold sea surface temperatures, so the surface ocean can remain a sink for atmospheric heat as long as the surface ocean is colder than the lower atmosphere. Ocean circulation carries the absorbed heat away from the surface waters, which also maintains cold sea surface

temperatures (Armour et al., 2016; Morrison et al., 2016). Northward heat transport is controlled by passive advection and eddy processes (Morrison et al., 2016). Processes that weaken Southern Ocean convection can also reduce ocean heat gain. For example, sea ice retreat at the sea ice edge or within polynyas leads to weakening convection in the Southern Ocean by freshening the surface waters (Bitz et al., 2006), which reduces the drawdown of heat from the atmosphere into the ocean (Newsom et al., 2016).

For roughly half the year the Southern Ocean releases heat into the atmosphere via some of the same processes by which it absorbs heat. For example, mixing in the upper ocean facilitates heat loss to the atmosphere in the fall and winter (Gille et al., 2016) by more efficiently delivering heat stored in the deep ocean to the surface. Wintertime heat fluxes from the ocean to the atmosphere are often exacerbated by surface mixing caused by high winds and storms (Holte et al., 2012). Indeed, wind is one of the few ways that the oceanic and atmospheric mechanisms of Southern Ocean air-sea heat fluxes have been connected.

Few studies have focused on how the atmosphere itself can modulate Southern Ocean heat gain and loss. Winds play an important role by advecting cold and dry air from Antarctica over the ocean, reducing air temperature and humidity and driving turbulent heat fluxes from the ocean to the atmosphere (Doddridge et al., 2021; Ogle et al., 2018). By extension, the air-sea temperature and humidity gradients are also important in modulating heat gain and loss: the larger the gradient, the larger the heat flux. Another atmospheric property that modulates heat fluxes out of the ocean is static stability. Observations around the Southern Ocean indicate that the lower troposphere is generally unstable (Bharti et al., 2019), which is common when sea surface temperatures are warmer than the air temperature. An unstable lower troposphere promotes convection at the ocean surface and enhances the flux of latent and sensible heat out of the ocean. The influence of other atmospheric properties on mechanisms and magnitude of Southern Ocean air-sea fluxes are still unknown.

Clouds, in particular, may be an important factor in determining the magnitude and seasonality of anomalous Southern Ocean heat gain and loss. Why? First, the Southern Ocean is, on average, the cloudiest region in the world. Annual mean total cloud cover typically exceeds 80% (Huang et al., 2012; Naud et al., 2014; Warren et al., 1988), mostly with cloud tops below 5 km (Haynes et al., 2011), making them an important factor in the energy budget of the Southern Ocean. Seasonal mean cloud cover between 50° and 70°S is fairly consistent (Mace & Zhang, 2014), though observations are sparse during the winter due to satellites' difficulty observing clouds in the dark seasons. The Southern Ocean is consistently cloudy due to many environmental factors, including frequent storms, strong cyclonic winds around the Antarctic continent, and bioavailability of cloud condensation nuclei (e.g., Kelleher & Grise, 2019; McCoy et al., 2015). Observations report that low-topped clouds have an optical depth between approximately 2 and 9 (Haynes et al., 2011) and have a high occurrence of supercooled liquid water (Lawson & Gettelman, 2014; Mace et al., 2020). Given the persistent cloud cover of the Southern Ocean, it is reasonable to assume that clouds play a role in Southern Ocean heat uptake.

Second, clouds have a known radiative effect on the surface. Clouds cool the surface by reflecting shortwave radiation away and warm the surface by downward emission of longwave radiation. Low clouds and clouds containing supercooled liquid water contribute the most to high latitude clouds' surface radiative effects (Shupe & Intrieri, 2004). Over the Southern Ocean, the mean net cloud radiative effect is negative, indicating that clouds generally cool the surface (Wang et al., 2020). Climate models have a known low bias in cloud liquid water path over the Southern Ocean (Bodas-Salcedo et al., 2014, 2016; Hyder et al., 2018; Vergara-Temprado et al., 2018), however, indicating that models may underestimate clouds' radiative effect on the Southern Ocean. Inaccurate representations of Southern Ocean clouds and their relationship with air-sea heat transport limits our ability to predict future climate change.

Third, climate model experiments have shown that interactions between clouds and the ocean can mitigate the pace of transient climate change and increase climate sensitivity through clouds' radiative feedbacks (Rose & Rayborn, 2016; Trossman et al., 2016). Models from the Coupled Model Intercomparison Project Phase 6 (CMIP6; Eyring et al., 2016) often agree that between the first and last 20 years of the historical period (1994–2014 minus 1850–1870), the peak in Southern Ocean heat uptake occurs near 60°S (Figure 1a). There is very little difference in total cloud cover between the beginning and end of the historical period (Figure 1b), but the peak in many models' ocean heat uptake often occurs near the same latitude as the peak in the Southern Hemisphere's vertically integrated cloud liquid water (Figure 1c). While the CMIP6 models do not always agree on the location or magnitude of cloud liquid water path, the general agreement that the peaks in ocean heat uptake occur near the peaks

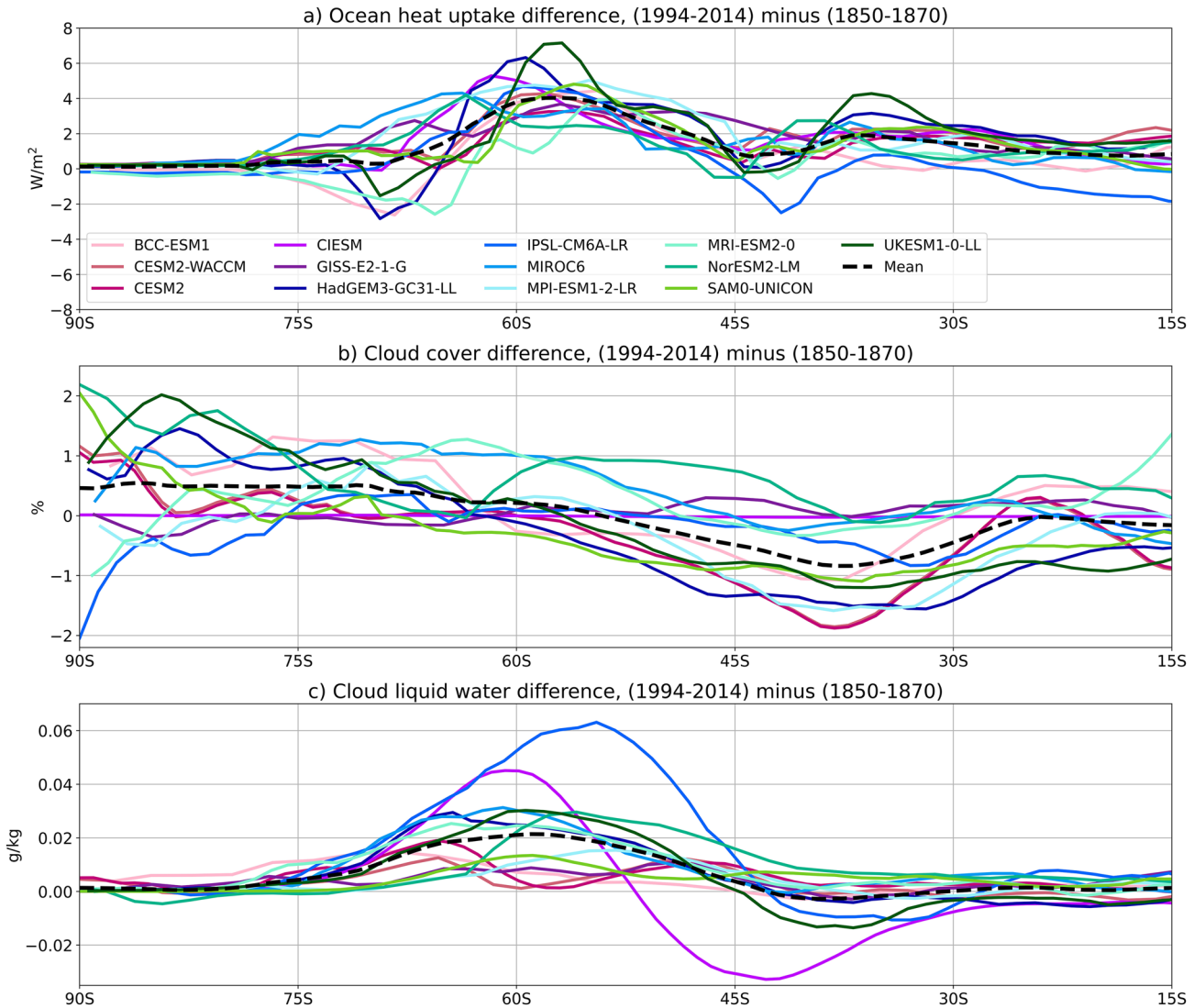

Figure 1. Difference in meridional mean (a) ocean heat uptake, (b) total cloud cover, and (c) vertically integrated atmospheric cloud liquid water in CMIP6 models' historical runs between 1994–2014 and 1850–1870 (Eyring et al., 2016).

in cloud liquid water path motivates us to understand how interactions between cloud properties and the ocean enhance or mitigate the oceanic mechanisms of Southern Ocean heat uptake.

Finally, clouds have a known relationship with atmospheric stability, a factor that influences heat release from the ocean (see above). Increased atmospheric stability reduces atmospheric convection at the surface, which suppresses turbulent heat fluxes—and therefore heat loss—out of the ocean. In the mid-latitudes, a more stable atmosphere has been linked to increased cloud cover (Klein & Hartmann, 1993; Wood & Bretherton, 2006). Given the observed relationship between clouds and stability, and the known cloud radiative effect at the surface, clouds may influence surface turbulent heat fluxes as well as surface radiative heat fluxes.

Due to the Southern Ocean's challenging weather conditions, air-sea fluxes and clouds can be difficult to observe, especially during the winter. Observations from ship cruises and ocean buoys, while valuable, lack the necessary spatial and temporal coverage to study the relationship between clouds and ocean heat uptake. Satellite observations do achieve a more complete areal coverage of the Southern Ocean, but lack a long enough data record for robust statistics (>30 years), and can provide only a partial picture of the processes relevant to understanding the energy budget. Certain types of observations are especially problematic. The largest errors in Southern Ocean surface heat budget calculations come from uncertainty in air-sea fluxes (Dong et al., 2007), due to sparse in situ

observations and difficulty in calibrating remote sensors (e.g., Bourassa et al., 2013; Josey et al., 1999; Swart et al., 2019). Southern Ocean studies that use air-sea fluxes, therefore, commonly rely on global atmospheric reanalyses (e.g., Liu et al., 2011), which is the method we employ here.

In this study, we attempt to understand the roles that atmospheric processes may play in mediating air-sea heat transport in the Southern Ocean. We examine the relationship between clouds and the mechanisms of Southern Ocean heat gain and loss in two reanalyses over the period 1979–2020. The paper is organized as follows: Section 2 describes the reanalysis data sets and methods. Section 3 begins with an analysis of the spatial patterns, seasonality, and variability of Southern Ocean heat gain and loss from 1979 to 2020. We next assess the relationship between seasonal mean air-sea heat transport and atmospheric states like cloudiness and stability, and how changes in atmospheric states may affect surface radiative and turbulent fluxes. Section 3 concludes with an analysis of the environmental conditions contributing to the observed change in atmospheric states. Section 4 discusses the physical reasoning behind the observed impact of clouds on Southern Ocean heat gain and loss, as well as our results' implications for the representation of Southern Ocean clouds in climate models. Section 5 presents the summary and conclusions.

2. Data and Methods

2.1. ERA5 and JRA-55 Reanalysis Data

To identify the relationships between clouds and air-sea heat transport in the Southern Ocean, we use the ECMWF ERA5 (Hersbach et al., 2020) and the Japanese 55-year Reanalysis (JRA-55; Kobayashi et al., 2015) global atmospheric reanalysis data sets. Our choice of reanalyses was dependent on two criteria. First, the reanalyses needed to have all the fields for calculating ocean heat uptake and for analyzing atmospheric properties like cloud liquid water path. Second, the reanalyses needed to have physically reasonable representations of all relevant fields, especially surface fluxes, over at least the last 40 years. Both ERA5 and JRA-55 have all the relevant fields for this study in a continuous record since 1979, and have relatively small known biases in surface fluxes and clouds. Compared with available observations around the Southern Ocean, ERA5 slightly underestimates both cloud cover and the longwave radiative effect (Wang et al., 2020), while JRA-55 also underestimates cloud cover (Tsujino et al., 2018). Both reanalyses provide low cloud cover as well as total cloud cover. Low clouds in ERA5 are defined as clouds that occur on model levels with pressure more than 0.8 times the surface pressure (Hersbach et al., 2020), so over the Southern Ocean low clouds usually occur on levels with pressure greater than 800 mb. Low clouds in JRA-55 are defined similarly, and occur on model levels with pressure greater than 850 mb (Kobayashi et al., 2015).

We use monthly mean values from 1979 to 2020. ERA5 has a horizontal resolution of roughly 0.28° (approximately 31 km) and 137 atmospheric levels from the surface to 0.01 hPa. ERA5 monthly means are calculated from hourly output. JRA-55 data are provided on a reduced Gaussian grid at a TL319 horizontal resolution (approximately 55 km) and 60 atmospheric levels from the surface to 0.1 hPa. JRA-55 monthly mean values are calculated from 3- or 6-hourly output. Both reanalyses use data that are assimilated from satellite, ship-based, and ocean buoy observations, using a 4D-Var assimilation scheme.

2.2. Assessing Relationships Between Southern Ocean Heat Uptake and Atmospheric States

Since the Southern Ocean has a strong seasonal cycle in heat gain and loss, we use a single term to refer to the transport of heat between the atmosphere and ocean: Southern Ocean heat uptake (SOHU). SOHU is negative if heat is escaping the ocean (i.e., the ocean is cooling), or positive if the ocean is absorbing heat (i.e., the ocean is warming). In our study, it is a measure of how much heat and energy are transported between the ocean and the atmosphere over a given time period. We adopt the convention that the sign of net surface radiative fluxes (the sum of shortwave, F_s, and longwave, F_L, radiative fluxes) is positive into the surface, and the sign of turbulent heat fluxes (the sum of latent, F_{LA}, and sensible, F_{SN}, heat fluxes) is positive out of the surface. SOHU is defined as the difference between net radiative and turbulent fluxes at the surface at every ocean grid point (Equation 1). Since the direction of turbulent heat fluxes changes depending on whether heat is going in or coming out of the ocean, the turbulent heat fluxes are (by our convention) positive in the fall and winter and negative in the spring and summer. The data used in this study are monthly means, so SOHU is calculated and reported as a monthly mean as well.

$$\mathrm{SOHU}(x, y, t) = F_s + F_L - F_{LA} - F_{SN} \quad (1)$$

For most of our analysis, we assess the relationship between atmospheric variables and the SOHU index, which is the annual or seasonal mean ocean heat uptake area averaged over all ocean grid cells between 45° and 65°S in every year. Where we report the relationship between atmospheric variables and total cloud cover index, the total cloud cover index is the seasonal mean total cloud cover averaged over all ocean grid cells between 45° and 65°S in every year. Both the SOHU and total cloud cover indices are detrended before further analysis.

Due to the established relationships between clouds and atmospheric stability (see Section 1), we also assess the relationship between ocean heat uptake and lower tropospheric stability. Atmospheric stability is defined here as the difference in potential temperature between 800 mb and the surface. This definition of atmospheric stability is based on Klein and Hartmann (1993) and adapted based on Naud et al. (2020) to more accurately capture the relationship between Southern Ocean clouds and atmospheric temperature.

For each variable we calculate seasonal anomalies by subtracting the long-term (1979–2020) seasonal climatology from seasonal mean values in winter (June–July–August), spring (September–October–November), summer (December–January–February), and fall (March–April–May). To assess the relationship between SOHU and atmospheric variables, we use a linear regression method following the approach in Deser et al. (2017) as follows: for the relationship between seasonal atmospheric variables and SOHU, we find the linear fit of the seasonal atmospheric variable anomaly at every grid point, $V_{S,y}$, to the seasonal SOHU index, $U_{S,y}$, where V is the atmospheric variable of interest, U is the SOHU index, S represents a seasonal quantity, and y represents that the quantity specifies a particular year. Then our linear fit is:

$$V_{S,y}(\mathrm{lat}, \mathrm{lon}) = A(\mathrm{lat}, \mathrm{lon}) + B(\mathrm{lat}, \mathrm{lon}) * U_{S,y} \quad (2)$$

Upon solving for A and B, we show the spatial pattern of the atmospheric variable when the annual SOHU index is 2 SDs above the climatological mean. For the relationship between seasonal and annual mean SOHU, we use Equation 2 above, substituting the seasonal SOHU index for the annual SOHU index and the seasonal atmospheric variable anomaly for the seasonal SOHU anomaly.

Finally, we calculate and report Pearson correlations to show the strength of the relationships. When the correlation coefficient is reported for the entire Southern Ocean, it refers to the spatial correlation between two 2D fields for all ocean grid cells between 45° and 65°S, area-weighting to account for differences in grid cell area. When the coefficient is reported for different sectors, the coefficient still refers to a spatial correlation but only for a certain sector of the Southern Ocean between 45° and 65°S. While some correlation coefficients and significance are reported in the text for emphasis, correlations for the relationships described below, in all sectors and over the entire Southern Ocean, are reported in a Table S1 in Supporting Information S1

3. Results

3.1. Annual and Seasonal Mean Southern Ocean Heat Uptake, 1979–2020

We first present the annual mean SOHU from 1979 to 2020 in ERA5 and JRA-55 (Figure 2); a positive mean value indicates net heating of the upper ocean, while a negative mean value indicates a net cooling. Though the focus of this study is on seasonal relationships, we use the annual mean SOHU to confirm that ERA5 and JRA-55 are spatially and quantitatively consistent. In Figures 2a and 2b, the Southern Ocean is separated into six sectors to more easily identify regions of interest. The sectors are as follows: (a) South Atlantic Ocean (SAO), (b) African (AFR), (c) South Indian Ocean (SIO), (d) Australian (AUS), (e) South Pacific Ocean. (SPO), and (f) South American (SAM). The dotted line at 65°S represents the poleward boundary of defining our SOHU index. In the annual mean, ERA5 (Figure 2a) and JRA-55 (Figure 2b) have a very similar spatial pattern of ocean heat uptake. In every sector the Pearson correlation between ERA5 and JRA-55 is above 0.85, and across the entire Southern Ocean from 45° to 65°S the correlation is 0.90. In both reanalyses ocean heat uptake is most positive (i.e., the most net heating) in the South Atlantic Ocean, African, and South Indian Ocean sectors (sectors a-c), up to nearly 110 W/m^2. In both reanalyses ocean heat uptake is most negative (i.e., the most net cooling) in the South Pacific Ocean and South America sectors (sectors e, f)

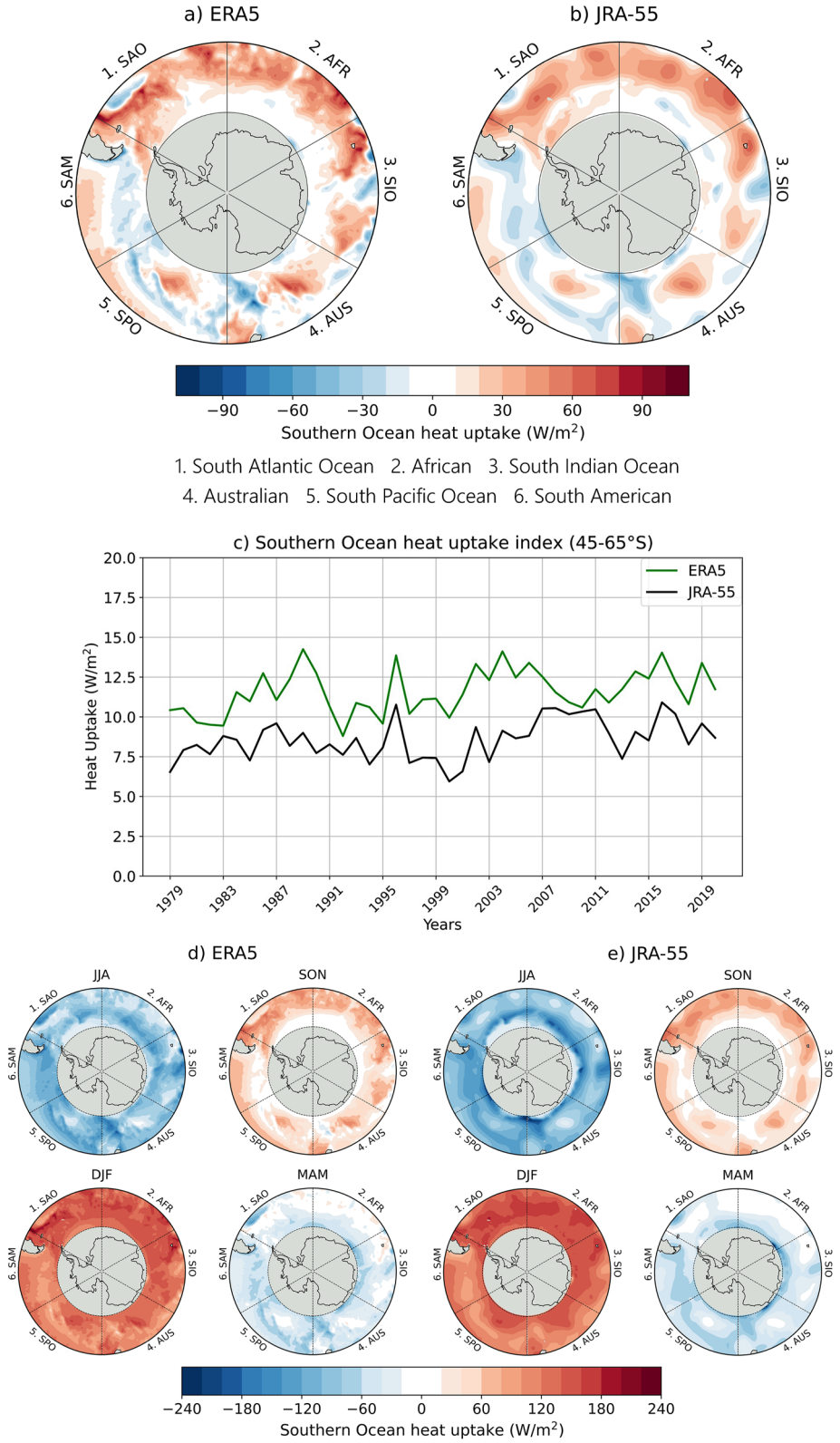

Figure 2. Annual mean Southern Ocean heat uptake in (a) ERA5 and (b) JRA-55 from 1979 to 2020. Sectors are numbered and labeled for ease of identification in the text. The dotted line at 65°S represents the poleward boundary that defines the Southern Ocean heat uptake index. (c) Annual mean time series of the Southern Ocean heat uptake index in ERA5 (green) and JRA-55 (black) from 1979 to 2020. Here, the Southern Ocean heat uptake index is the annual mean ocean heat uptake averaged across 45°–65°S. Seasonal mean Southern Ocean heat uptake in (d) ERA5 and (e) JRA-55 from 1979 to 2020.

Overall, in the annual mean the Southern Ocean absorbs more heat than it releases in both ERA5 and JRA-55. The annual mean SOHU index is positive in every year (Figure 2c), though the SOHU index in ERA5 is always larger than in JRA-55. There is no statistically significant trend in either reanalysis. The Pearson correlation between time series is 0.48 ($p < 0.05$), as the time series also do not show the same direction of change in every year—that is, in years when the SOHU index increases in ERA5, it does not necessarily increase in JRA-55. The positive annual mean Southern Ocean heat uptake masks a strong seasonal cycle of heat gain and loss. When the annual mean heat uptake is broken down into its seasonal components (Figures 2d and 2e), it is clear that in the seasonal mean the Southern Ocean gains heat in the spring and summer (positive SOHU), and loses heat to the atmosphere in the fall and winter (negative SOHU).

Given the strong seasonal cycle of heat gain and loss in the Southern Ocean (Figures 2d and 2e), we now consider the heat budget of the Southern Ocean by examining spatial variations of SOHU as a function of season, by regressing the annual mean SOHU index (Figure 2c) against the year-by-year anomalies in the net surface flux by season about the appropriate 42-year seasonal mean. Figure 3 displays the seasonal SOHU anomaly during very strong SOHU years ($U'_{A,y} = +2\sigma$) compared to the seasonal climatological SOHU. That is, Figure 3 shows which seasons have the largest net surface heat flux anomalies when annual SOHU is anomalously strong. From Figures 2d and 2e we know that the Southern Ocean gains heat in the spring and summer and loses heat in the fall and winter. Therefore, a positive SOHU anomaly in the spring and summer (fall and winter) means that the Southern Ocean gains more (or loses less) heat in years of strong SOHU. In years when annual mean SOHU was higher than average, local seasonal mean anomalies are up to 32 Wm^{-2} higher or lower than its local seasonal average (Figures 3a and 3b). Both reanalyses suggest that seasonal mean SOHU anomalies are not homogenous around the Southern Ocean. In ERA5 (Figure 3a), the SOHU anomalies are positive in the African sector in every season; in the Australian sector the ocean gains more heat in the spring and summer but loses more heat in the fall and winter. In JRA-55 (Figure 3b), the South Pacific Ocean sector loses less heat in the winter (positive SOHU anomaly) but has almost no net change in the summer and fall.

When the seasonal mean heat uptake anomaly is averaged between 45° and 65°S, it is clear that all seasonal anomalies are positive. In ERA5 (Figure 3c), the largest spatially averaged seasonal mean heat uptake anomaly occurs in the spring. In JRA-55 (Figure 3d), the largest spatially averaged seasonal mean heat uptake anomaly occurs in the winter. In both reanalyses, the smallest SOHU anomalies occur in the summer, so anomalously high annual mean SOHU is not controlled by an increase in heat gain during summer. Importantly, in years when the annual mean SOHU is 2 SDs above the climatological mean, the Southern Ocean loses *less* heat in the fall and winter and gains *more* heat in the spring. While the contributions of seasonal mean SOHU in winter, spring, and fall are important to annual mean SOHU, we restrict our analysis only to winter and spring to conserve space in the text and focus on the seasons with the largest SOHU anomalies in both ERA5 and JRA-55.

3.2. Changes in Winter and Spring Clouds During Anomalously Strong Ocean Heat Uptake

A similar decomposition of other fields according to regression on strong SOHU years is revealing. We now assess the relationship between seasonal SOHU and cloud cover by looking at the change in cloud structure anomalies (Figure 4). Between 45° and 60°S, zonal mean winter cloud cover increases by up to 2.4% below 900 mb (Figures 4a and 4b) during anomalously high winter SOHU in both ERA5 and JRA-55. However, ERA5 shows a slight increase in mid-level cloud cover (from 900 to 650 mb) while mid-level cloud cover decreases in JRA-55. In both reanalyses, the largest increase in wintertime low-level cloud cover occurs between 50° and 60°S. During anomalously high winter SOHU, zonal mean specific humidity increases through the lower atmosphere (contours). The largest increase in specific humidity, approximately $6*10^{-4}$ g/kg, is around 55°S, corresponding to the largest increase in cloud cover.

As in winter, low-level cloud cover also increases during spring (Figures 4c and 4d), albeit by only approximately 1.3%. The vertical structure of spring cloud cover anomalies differs between ERA5 and JRA-55. At higher (lower) latitudes, cloud cover increases (decreases) slightly through 650 mb in ERA5 (Figure 4c). Above approximately 900 mb, cloud cover decreases slightly in JRA-55 (Figure 4d). During anomalously high spring SOHU, zonal mean specific humidity increases throughout the lower atmosphere, but the largest increases occur

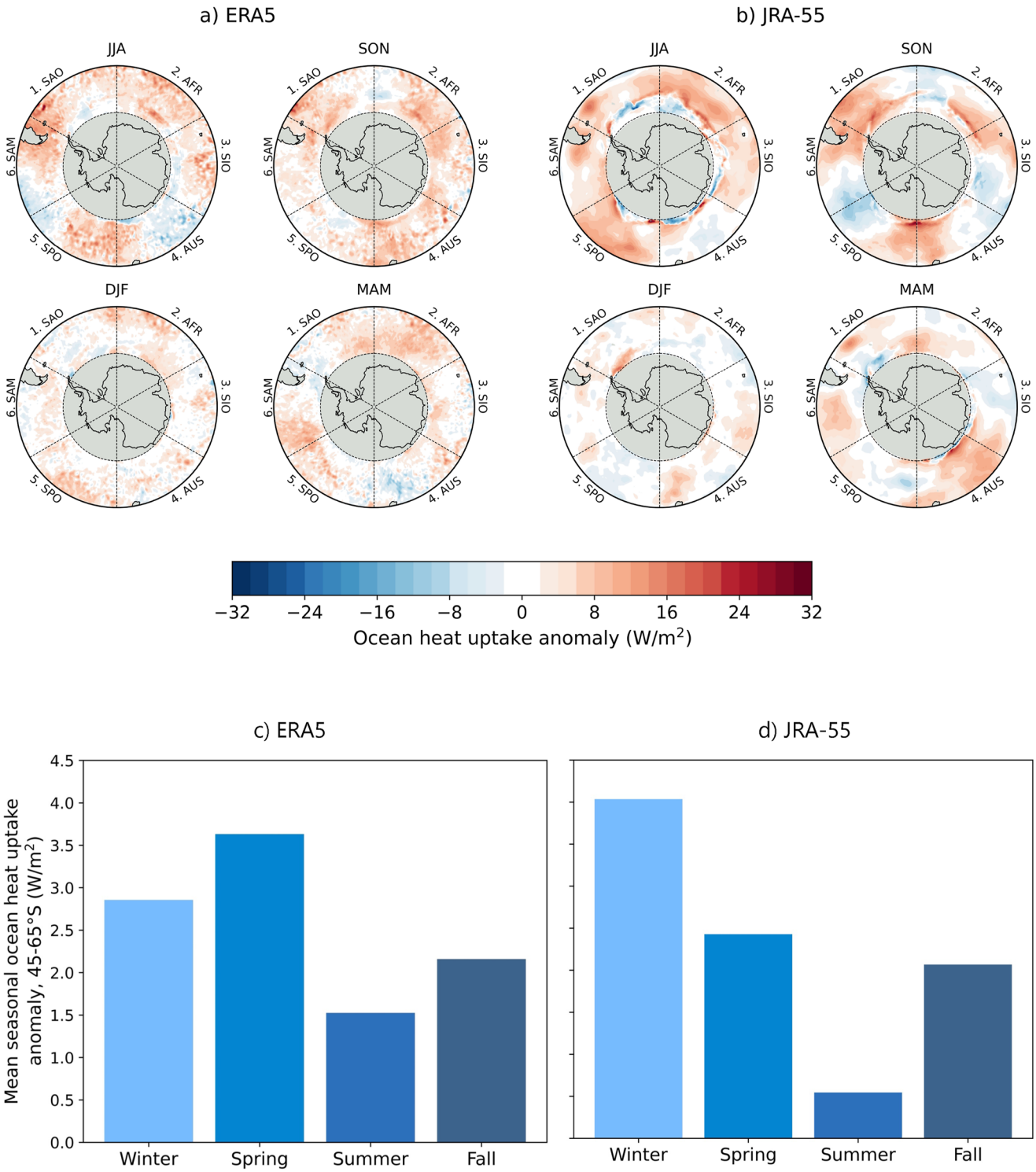

Figure 3. Regressions of seasonal mean Southern Ocean heat uptake on seasonal Southern Ocean heat uptake index for (a) ERA5 and (b) JRA-55. The dotted line at 65°S represents the poleward boundary of the Southern Ocean heat uptake index. Ocean heat uptake anomalies are relative to the seasonal mean Southern Ocean heat uptake shown in Figure 2. Seasonal mean ocean heat uptake anomalies in (a) and (b) averaged over the Southern Ocean (45°–65°S) for (c) ERA5 and (d) JRA-55.

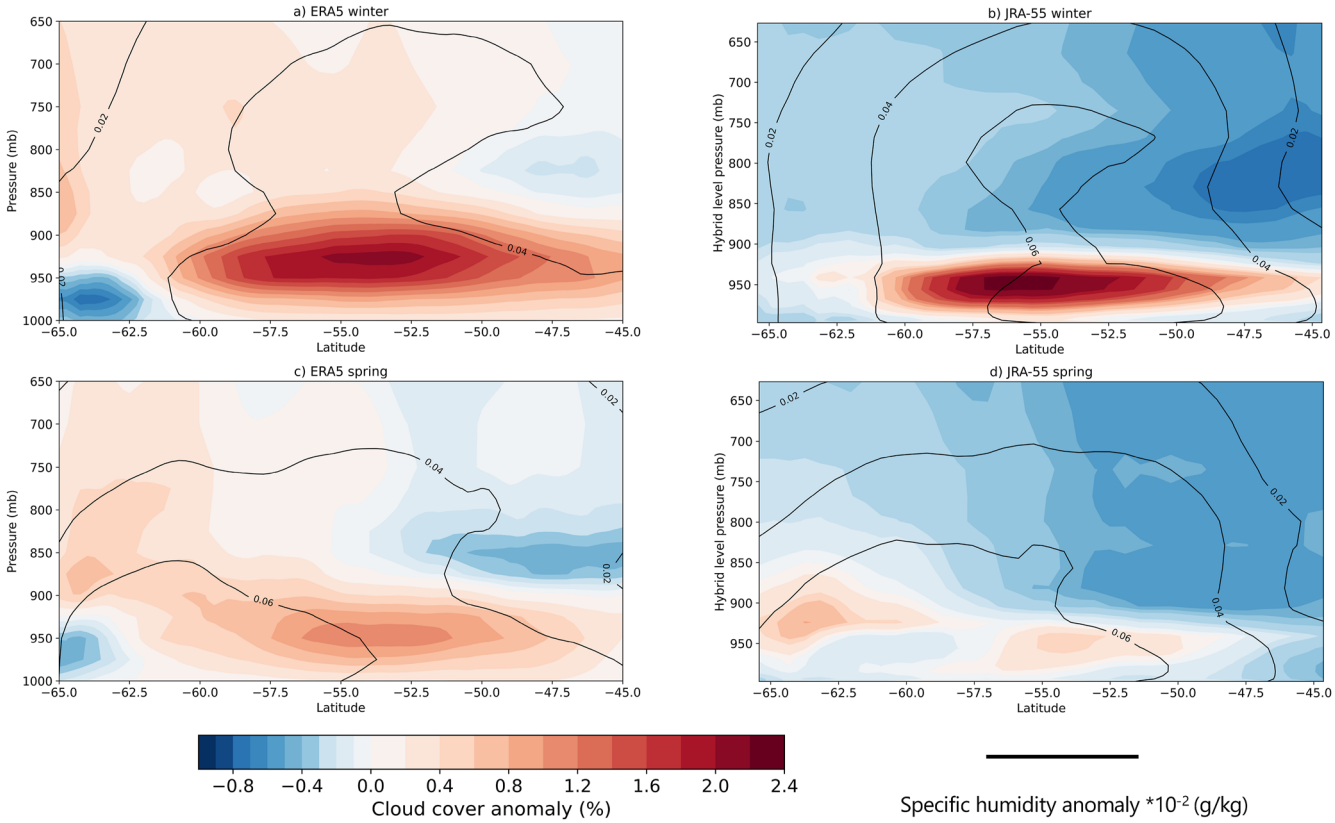

Figure 4. Regression of seasonal, zonal mean vertical cloud cover on seasonal Southern Ocean heat uptake index for (a) ERA5 winter, (b) JRA-55 winter, (c) ERA5 spring, and (d) JRA-55 spring. Shading is the cloud cover regression. Contours are the regression of seasonal, zonal mean specific humidity on seasonal Southern Ocean heat uptake index (Figure 3).

at slightly higher latitudes than they do in the winter—between approximately 52° and 65°S. While the most positive specific humidity anomalies do occur around the same height as the most positive cloud cover anomalies, the greatest specific humidity anomalies are generally poleward of the low-level cloud cover maximum (compare the $6*10^{-4}$ g/kg specific humidity anomaly contour to the cloud cover anomaly in Figure 4c).

Since the largest changes in cloud cover occur near or below 900 mb (Figure 4), we next assess the relationship between low-level cloud cover and SOHU across the entire Southern Ocean during winter and spring (Figure 5). We find that regional low cloud cover increases by up to 7% compared to its respective winter and spring climatological value. Wintertime cloud cover increases in every sector except for the Australian sector in ERA5 (Figure 5a). The relationship between low cloud cover and SOHU (contours) is also strongest in the Australian sector: the correlation of regressed cloud cover against regressed SOHU is 0.58. In the South Pacific Ocean sector, where low cloud cover anomalies are largest in ERA5, the correlation between clouds and SOHU is quite small (0.07 correlation) even though this is a region of large positive SOHU anomalies. While cloud cover increases across the entire South Pacific Ocean sector, there is a region of negative SOHU anomalies adjacent to the South American sector. The discrepancy between positive cloud and negative SOHU anomalies over this region likely leads to the very small correlation over the whole South Pacific Ocean sector. Wintertime low cloud cover increases in every sector in JRA-55 (Figure 5b), with the largest positive cloud cover anomalies in the South Pacific Ocean sector. Here, positive cloud cover anomalies are also spatially correlated with the most positive winter SOHU anomalies (0.55 correlation). Over the entire Southern Ocean, the correlation between low cloud cover and SOHU anomalies is 0.36 (ERA5) and 0.31 (JRA-55). Positive cloud cover and SOHU anomalies do not precisely overlap, which is evidenced by the low overall correlation; we overlay the heat uptake anomalies to show that winter clouds and SOHU are related, but that clouds are not the most important atmospheric driver of SOHU.

The relationship between springtime low clouds and SOHU (Figures 5c and 5d) is less coherent than the wintertime relationship. The spring cloud cover anomalies are smaller than in winter and are less uniform around the

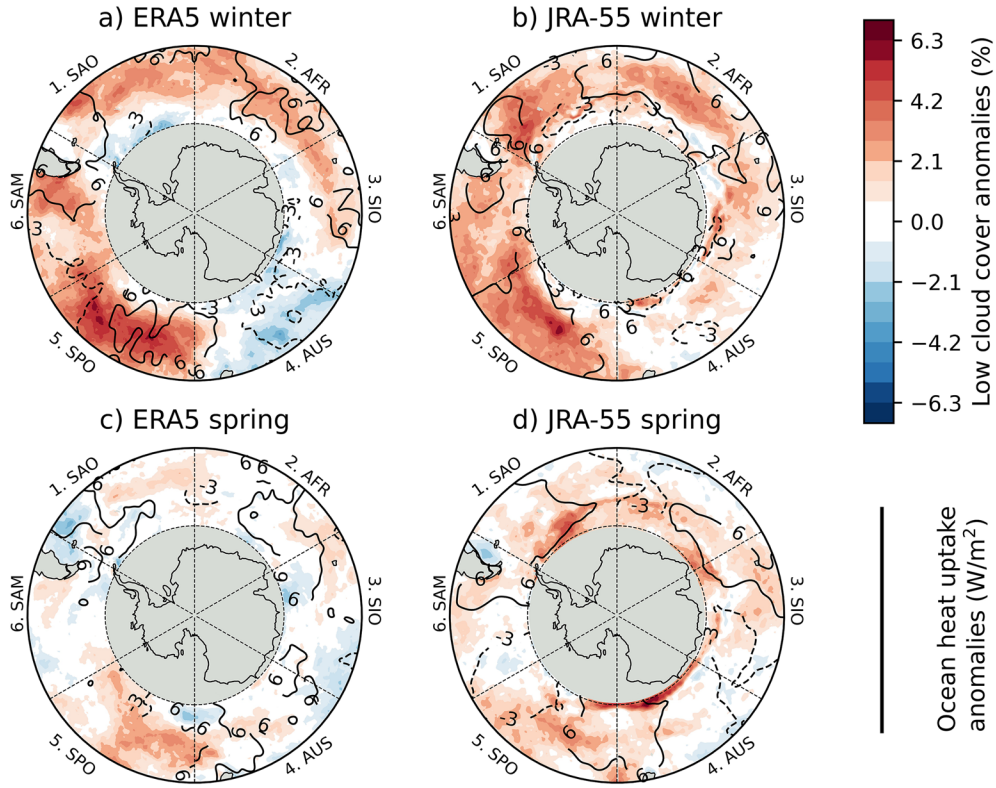

Figure 5. Regression of seasonal mean low cloud cover on seasonal Southern Ocean heat uptake index for (a) ERA5 winter, (b) JRA-55 winter, (c) ERA5 spring, and (d) JRA-55 spring. Shading is the cloud cover regression. Contours are the regression of seasonal mean Southern Ocean heat uptake on the annual mean Southern Ocean heat uptake index (Figure 3).

Southern Ocean. The mean cloud cover change by sector is negligible (within 0.5% of zero) everywhere except the South Pacific Ocean sector in ERA5 (Figure 5c) and in the South Pacific and South Atlantic Ocean sectors in JRA-55 (Figure 5d). Unlike in winter, in spring ERA5's cloud cover and SOHU anomalies are weakly anti-correlated, with a correlation of −0.21 across the Southern Ocean. Springtime JRA-55 cloud cover anomalies are weakly linked to regions to positive SOHU anomalies (0.22 correlation). These weak springtime correlations suggest that clouds have a stronger relationship to winter SOHU than to spring SOHU.

When Southern Ocean heat uptake is high, clouds are not only more frequent but are also contain more liquid water. Figure 6 shows the regression of cloud liquid water path on seasonal mean SOHU index. Cloud liquid water path is normalized by the total cloud cover before performing any analysis, so positive anomalies in Figure 6 indicate an increase in cloud liquid water and not just an increase in cloud cover (Figure 5). In the winter, both ERA5 (Figure 6a) and JRA-55 (Figure 6b) show positive cloud liquid water path anomalies everywhere except the Australian sector, with the largest positive anomalies in the South Pacific Ocean and South American sectors. There is a 0.31 (0.42) correlation between cloud liquid water path and SOHU (black contours) across the entire Southern Ocean in ERA5 (JRA-55). Cloud liquid water path also increases during anomalously high spring SOHU (Figures 6c and 6d), though the spring anomalies are smaller and much more heterogeneous than the winter anomalies. In contrast with the winter, cloud liquid water path increases in the Australian sector in both reanalyses but decreases in the South Indian Ocean sector. Statistically the mean cloud liquid water path anomaly in the South Indian Ocean sector of ERA5 and JRA-55 is zero (<0.001 $g/m^3/\%$). In spring, there is no statistical relationship between cloud liquid water path and SOHU anomalies in ERA5, but a positive relationship in JRA-55 (0.39 correlation) across the entire Southern Ocean.

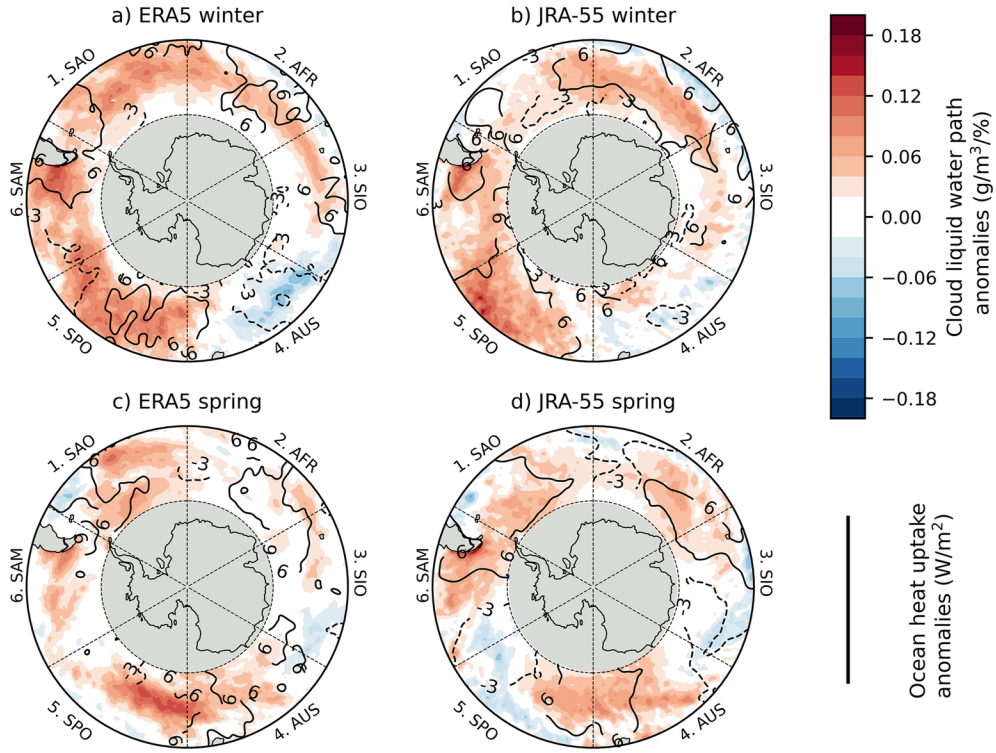

Figure 6. As in Figure 5 except for cloud liquid water path. Shading is the cloud liquid water path regression. The cloud liquid water path is normalized by total cloud cover before performing any analysis. Contours are the regression of seasonal mean Southern Ocean heat uptake on the annual mean Southern Ocean heat uptake index (Figure 3).

3.3. Evaluation of Surface Fluxes During Strong Winter and Spring Ocean Heat Uptake

We have established that clouds appear to covary with SOHU in both winter and spring. Clouds could impact SOHU through radiative mechanisms, turbulent mechanisms, or both. We now investigate each of these possibilities in turn.

First, Figure 7 shows the regression of seasonal net downward longwave flux (all-sky conditions minus clear-sky conditions) on the seasonal SOHU index. During anomalously high winter and spring SOHU, the net surface downward longwave flux increases by up to 5 W/m^2. As we are showing the difference in net longwave flux between all-sky and clear-sky conditions, longwave flux anomalies are associated with clouds and atmospheric properties that co-vary with clouds. Because clouds do not change independently of other atmospheric properties, such as humidity and temperature, we attribute the observed longwave flux anomalies to both clouds and to changes in the atmospheric state that accompany cloud changes. In both reanalyses (Figures 7a and 7b), the most positive wintertime longwave flux anomalies are closely correlated with positive cloud cover anomalies (solid contours). There is a 0.94 (0.71) correlation between net surface downward longwave flux and low cloud cover anomalies across the entire Southern Ocean in ERA5 (JRA-55). In the South Pacific Ocean sector, which has the largest mean net surface downward longwave flux anomalies in both reanalyses, the correlation between longwave flux and low cloud cover is 0.98 in ERA5 and 0.83 in JRA-55.

In contrast with winter, the cloud cover and liquid water path anomalies are smaller during spring, so the corresponding net downward longwave flux anomalies are also smaller. During the spring (Figures 7c and 7d), longwave flux anomalies due to cloud changes are almost negligible in much of the Southern Ocean. In each sector the mean longwave flux anomaly is less than 1 W/m^2. In both ERA5 and JRA-55, the largest increase in longwave flux is in the South Pacific Ocean sector. Even though their magnitude is not very large, longwave flux anomalies are still strongly correlated with cloud cover anomalies in ERA5 (0.82 correlation across the Southern Ocean), with the strongest positive relationship in the South Pacific Ocean sector (0.92 correlation). The relationship between longwave flux and clouds weakens slightly from the winter to the spring in JRA-55, with a 0.49

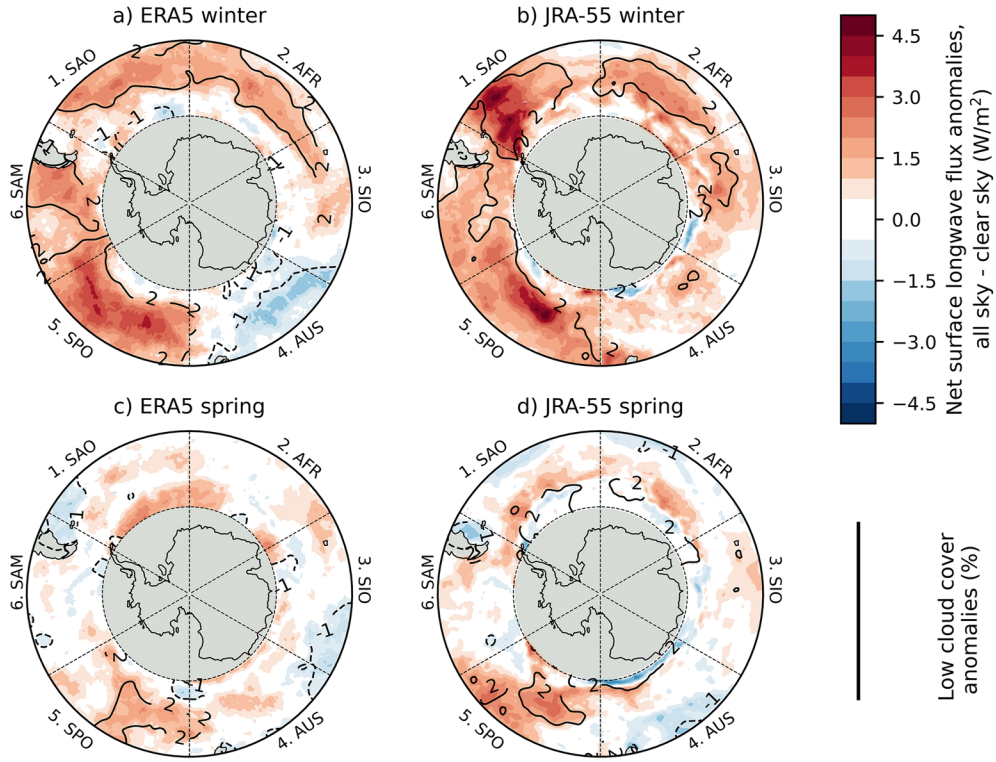

Figure 7. Regression of seasonal mean net downward longwave flux anomaly, all-sky minus clear-sky, on the seasonal Southern Ocean heat uptake index for (a) ERA5 winter, (b) JRA-55 winter, (c) ERA5 spring, and (d) JRA-55 spring. Shading is the longwave flux regression. Contours are the regression of seasonal low cloud cover on seasonal Southern Ocean heat uptake index (Figure 5).

correlation between springtime longwave flux and cloud cover across the entire Southern Ocean due to very weak relationships in the South Atlantic Ocean and Australian sectors We conclude that in both winter and spring, clouds (and the atmospheric states that accompany clouds) do contribute to SOHU by increasing downwelling longwave radiation at the surface.

Now we assess the possibility that clouds may also affect SOHU by mediating total turbulent heat fluxes (combined sensible and latent heat fluxes) out of the surface. During anomalously high winter and spring SOHU, turbulent heat flux anomalies are negative almost everywhere in the Southern Ocean compared to the winter and spring seasonal mean (Figure 8). Negative turbulent heat flux anomalies indicate that heat fluxes out of the ocean are reduced, so more heat remains in the ocean. During winter, turbulent heat fluxes are reduced by up to 25 W/m^2 in ERA5 (Figure 8a) and by up to 32 W/m^2 in JRA-55 (Figure 8b). In ERA5 the largest reduction is in the South Atlantic Ocean sector; in JRA55 the largest reduction is in the South Pacific Ocean sector. However, the reduction in turbulent heat fluxes is not uniform around the continent. Turbulent heat fluxes from the ocean to the atmosphere strengthen in the lower latitudes of the Australian sector and between the South Pacific Ocean and South American sectors; the increase in turbulent heat fluxes out of the ocean is larger in ERA5 than in JRA-55. In the spring turbulent heat fluxes are reduced by up to 24 W/m^2 in ERA5 (Figures 8c) and 20 W/m^2 in JRA-55 (Figure 8d). As in the winter, heat fluxes out of the ocean strengthen between the South Pacific Ocean and South American sectors in both reanalyses. The largest springtime reductions in turbulent heat fluxes occur between the South Pacific Ocean and Australian sectors.

Clouds do not appear to have a strong effect on total turbulent heat fluxes out of the ocean in either reanalysis in either season. While wintertime heat flux and cloud cover anomalies are anticorrelated across the entire Southern Ocean in ERA5 and JRA-55 (−0.31 and −0.16, respectively), the strongest relationship occurs in the Australian sector in ERA5. In the Australian sector, reduced cloud cover is linked to increased turbulent heat fluxes out of the ocean (−0.72 correlation). Reduced turbulent heat fluxes and positive cloud cover anomalies (solid contours) do often overlap in the spring, but regions of reduced heat flux and increased cloud cover are not statistically

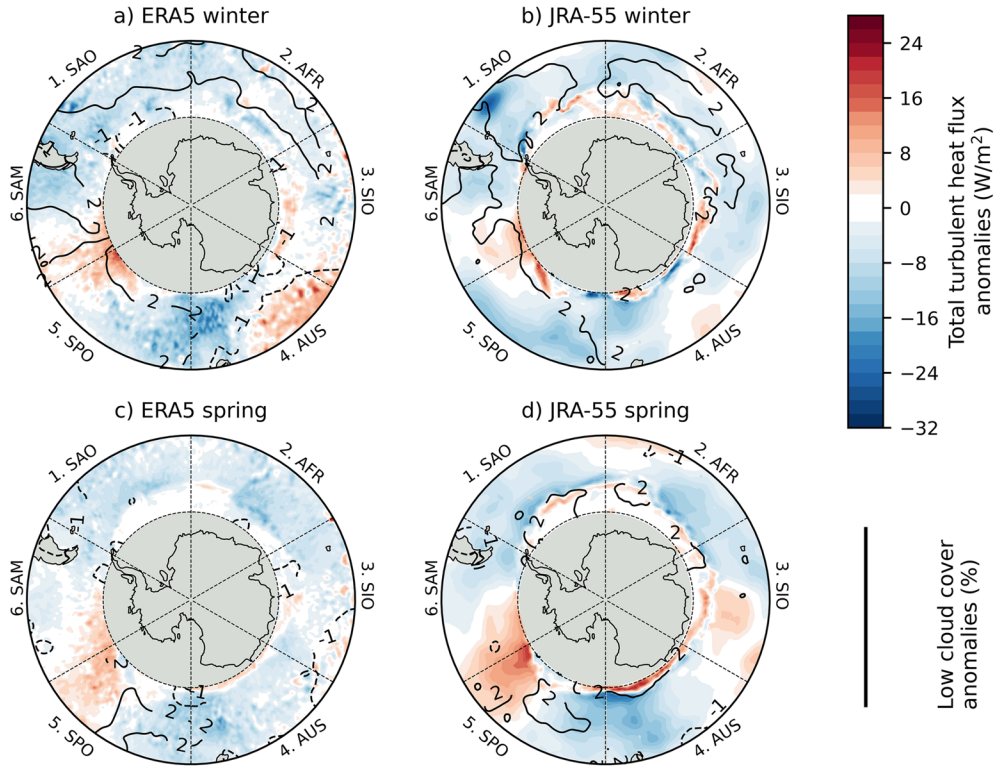

Figure 8. Regression of seasonal mean net turbulent heat fluxes on the seasonal Southern Ocean heat uptake index for (a) ERA5 winter, (b) JRA-55 winter, (c) ERA5 spring, and (d) JRA-55 spring. The sign convention is that turbulent heat fluxes are positive out of the ocean. Shading is the turbulent heat flux regression. Contours are the regression of seasonal low cloud cover on the seasonal Southern Ocean heat uptake index (Figure 5).

connected. Indeed, the correlation between heat flux and cloud cover anomalies is smaller than −0.05 in both reanalyses. Since the reduction of turbulent heat fluxes out of the ocean is so important for increasing SOHU, we next investigate other atmospheric processes besides clouds that may affect air-sea heat fluxes.

3.4. Atmospheric Conditions That Influence Cloud Cover and Fluxes

Although clouds do not directly mediate turbulent heat fluxes out of the ocean, the covariance between clouds and SOHU (Figures 4–6) leads us to investigate other connections between atmospheric conditions, clouds, and turbulent fluxes. The stability of the lower troposphere may connect clouds and turbulent fluxes. Therefore, we next present the relationship between atmospheric stability and SOHU.

During anomalously high SOHU, the lower atmosphere generally becomes more stable (Figure 9). In ERA5 (Figure 9a) and JRA-55 (Figure 9b), wintertime stability increases by up to 1.5 K everywhere across the Southern Ocean except in parts of the Australian sector. In the lower latitudes of ERA5's Australian sector the atmosphere becomes slightly less stable, by roughly 0.8 K. Near the Antarctic coast in JRA-55, around 65°S, atmospheric stability decreases by nearly 1.4 K. The differences in atmospheric stability between ERA5 and JRA-55 poleward of 65°S are due to changes in surface temperatures over sea ice, which affect the calculation of stability. Positive wintertime stability anomalies are collocated with positive low cloud cover anomalies (solid contours; Figure 5). Across the entire Southern Ocean, the correlation between stability and low cloud cover anomalies is 0.67 (0.52) in ERA5 (JRA-55). Only in ERA5 are negative stability anomalies also collocated with negative low cloud cover anomalies (dashed contours; 0.76 correlation). There is a very weak correlation between negative stability and positive cloud cover anomalies in the Australian sector of JRA-55 (−0.15).

Atmospheric stability anomalies have much more spatial variability in spring compared to winter, with more regions of negative anomalies, once again demonstrating how springtime relationships generally appear weaker than wintertime relationships. The largest increases in stability occur in the higher latitudes of the South Atlantic

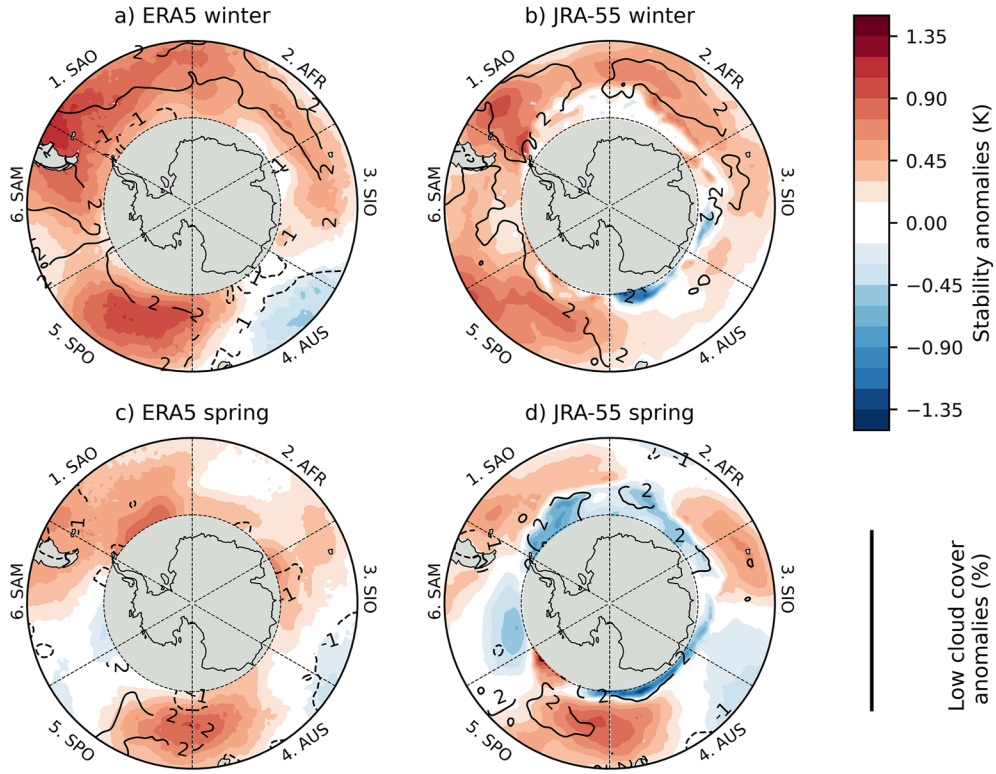

Figure 9. Regression of seasonal mean near-surface static stability (Θ_{800} - $\Theta_{surface}$) on the seasonal Southern Ocean heat uptake index for (a) ERA5 winter, (b) JRA-55 winter, (c) ERA5 spring, and (d) JRA-55 spring. Shading is the stability regression. Contours are the regression of seasonal low cloud cover on the seasonal Southern Ocean heat uptake index (Figure 5).

Ocean, the South Indian Ocean, and between the Australian and South Pacific Ocean sectors in ERA5 (Figure 9c) and JRA-55 (Figure 9d). In both reanalyses, stability decreases in the lower latitudes of the South Indian Ocean and Australian sectors. Stability also decreases near 65°S in the South Atlantic Ocean and Australian sectors in JRA-55, which is associated with a reduction in sea ice cover in these sectors (not shown). The relationship between atmospheric stability and low cloud cover, while strong in the winter, weakens in the spring: the correlation between stability and cloud cover anomalies is less than 0.28 for both reanalyses across the entire Southern Ocean. By sector, a positive relationship exists in the Australian sector of ERA5 (0.57 correlation); a negative relationship exists in the South Atlantic Ocean sector of JRA-55 (−0.61 correlation), dominated by the overlap between negative stability and positive cloud cover anomalies near 65°S.

Atmospheric stability may increase either because sea surface temperatures decrease or because tropospheric temperatures increase. Positive SOHU anomalies are linked to an increase in both low cloud cover (Figures 4 and 5) and atmospheric stability (Figure 9), so we expect to see a corresponding increase in atmospheric stability when we regress seasonal stability on the seasonal total cloud cover index. In other words, when cloud cover is anomalously high, we expect environmental conditions that correspond with an increase in atmospheric stability. Figure 10 shows the zonal mean temperature profile anomalies over ocean grid cells when total cloud cover between 45° and 65°S is anomalously high compared to the winter (Figures 10a and 10b) and spring (Figures 10c and 10d) seasonal mean. In both the winter and spring, atmospheric temperature increases more than surface temperature, up to 0.6 K above the seasonal mean. In ERA5 the surface is cooler or the same temperature in both seasons. In JRA-55 the surface does warm, though less than the atmosphere does, or remains the same temperature in both seasons. Overall, when total cloud cover is more than 2SDs above the 42-year seasonal mean, the upper atmosphere is warmer than the surface, which means that the atmosphere is also more stable. Notably, the winter and spring 800 mb temperature anomaly exceeds the surface temperature anomaly in both reanalyses, which is associated with increased atmospheric stability. The regression of zonal mean temperature profile anomalies on the SOHU index (not shown) provides the same results: when seasonal SOHU is anomalously strong, both

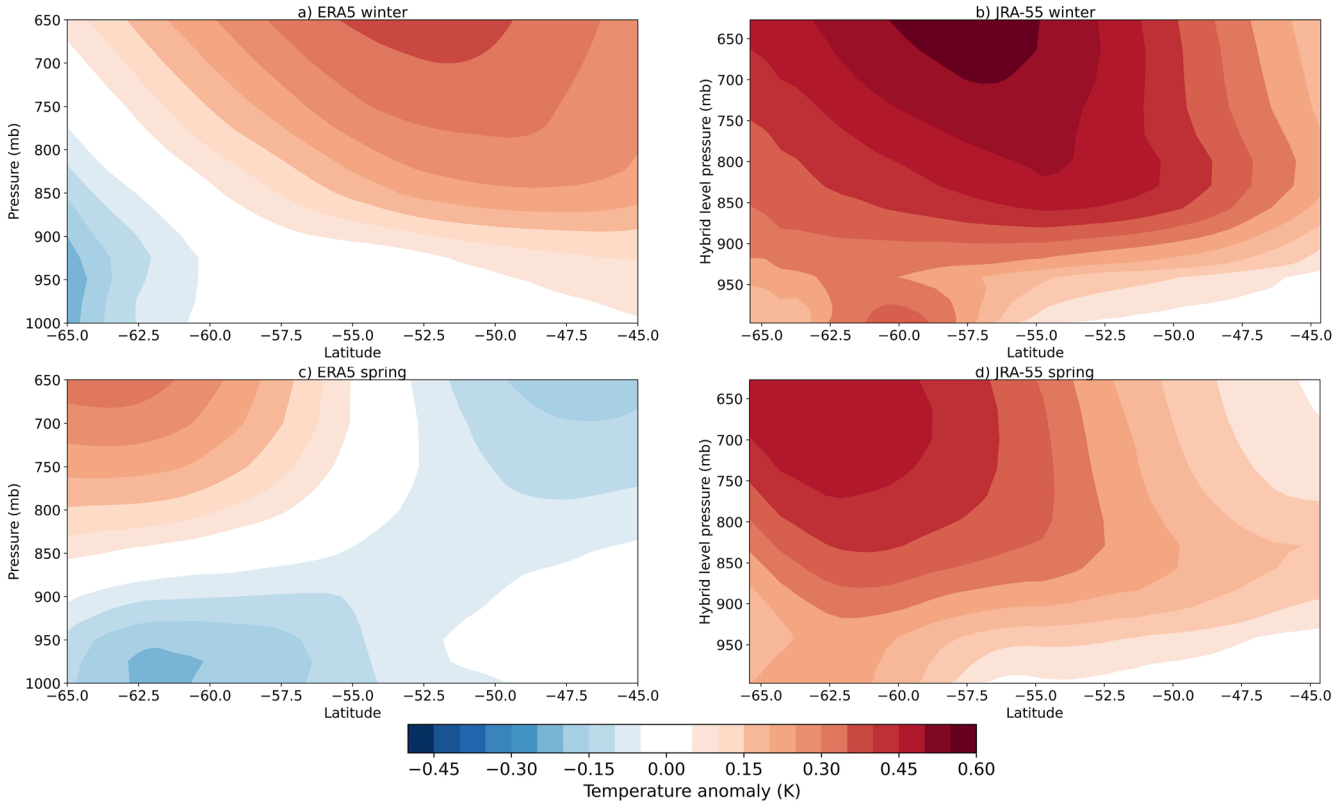

Figure 10. Regression of seasonal, zonal mean temperature on seasonal cloud cover index for (a) ERA5 winter, (b) JRA-55 winter, (c) ERA5 spring, and (d) JRA-55 spring. The seasonal cloud cover index is the mean total cloud cover between 45° and 65°S in winter and spring.

atmospheric and surface temperatures increase, but atmospheric temperatures increase faster, leading to greater static stability in the lower troposphere (between the surface and 800 mb).

3.5. Environmental Conditions During Anomalously High Winter and Spring Southern Ocean Heat Uptake

What mechanisms might explain the changes seen in clouds, atmospheric stability, and the atmospheric during anomalously high SOHU years and how do they impact heat uptake? The answer may be related to the synoptic conditions that exist when the ocean loses less heat in winter and gains more heat in spring. When the ocean loses less heat during winter, sea level pressure anomalies are in a wavenumber-3 pattern (Mo & White, 1985) in ERA5 (Figures 11a) and JRA-55 (Figures 11b), with lower pressure in the Australian sector, higher pressure in the South Pacific Ocean sector, and lower pressure in the South American sector. Note that the latitude boundaries in Figure 11 maps are 30°–65°S. Climatologically there is a low pressure trough poleward of 60°S (not shown here; see Rafael, 2004), with sea level pressure increasing concentrically toward the equator. The decrease in sea level pressure in the Australian and South American sectors is associated with a deepening of the climatic low pressure. Importantly for our study, changes in sea level pressure are linked to warm air intrusions, and changes in stability, uplift and subsidence, which affect clouds (and radiative fluxes) and turbulent heat fluxes out of the surface. In ERA5 the strongest relationship between sea level pressure and turbulent heat fluxes occurs in the Australian sector (−0.73 correlation), where reduced sea level pressure (i.e., more uplift and convection at the surface) is associated with increased heat fluxes out of the ocean. The strongest relationship in JRA-55 is in the South Atlantic Ocean sector, where increased sea level pressure (again connected to subsidence and reduced convection at the surface) is associated with suppressed heat fluxes (−0.62 correlation). Overall, wintertime sea level pressure anomalies are negatively correlated with turbulent heat flux anomalies (contours) everywhere except in the South Pacific Ocean sector in JRA-55, where they have a weak positive correlation of 0.15.

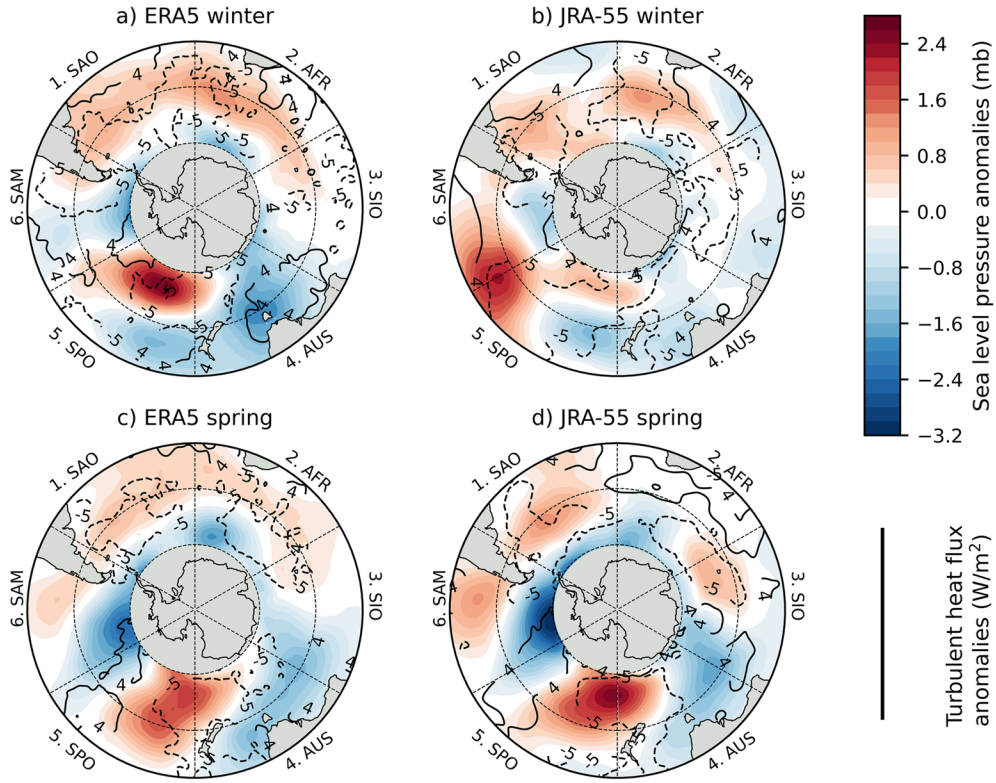

Figure 11. Regression of seasonal mean sea level pressure on the seasonal Southern Ocean heat uptake index for (a) ERA5 winter, (b) JRA-55 winter, (c) ERA5 spring, and (d) JRA-55 spring. Shading is the sea level pressure regression. Contours are the regression of seasonal turbulent heat fluxes on the seasonal Southern Ocean heat uptake index (Figure 8). The equatorward limit of Figure 11 is 30°S. The dotted lines at 45° and 65°S are the latitude limits of our defined Southern Ocean heat uptake index.

The sea level pressure anomaly pattern that occurs in winter still exists during spring (Figures 11c and 11d). The largest increase (decrease) in springtime sea level pressure occurs in the South Pacific Ocean (South America) sector in both ERA5 and JRA-55. As in the winter, sea level pressure and turbulent heat flux anomalies are negatively correlated across the entire Southern Ocean—a −0.47 correlation in ERA5 and −0.55 correlation in JRA-55. Regions of increased subsidence and uplift are associated with reduced and increased turbulent heat fluxes, respectively. In both reanalyses the strongest springtime relationship between sea level pressure and heat fluxes occurs in the South Pacific Ocean sector, where an increase in pressure is strongly correlated with a suppression of heat fluxes (−0.82 and −0.87 correlation in ERA5 and JRA-55, respectively).

Shifting spatial patterns of sea level pressure not only affect the transport of heat out of the ocean, but also the zonal transport of heat and water vapor, both of which affect atmospheric stability and cloud liquid water path. Figure 12 shows the regression of seasonal water vapor (green streamlines) and heat (purple streamlines) fluxes on the seasonal SOHU index. Arrows indicate the flux direction and the streamline thickness is proportional to the normalized seasonal flux magnitude. Flux direction and magnitude are calculated from and u- and v-components of ERA5 and JRA-55 water vapor and heat fluxes. As in Figure 11, the latitude boundaries in Figure 12 maps are 30°–65°S. In both the winter (Figures 12a and 12b) and spring (Figures 12c and 12d), the largest increases in sea level pressure (Figure 11) cause anomalous anticyclonic motion that bring heat and water vapor into the eastern edge of the South Pacific Ocean sector from lower latitudes. The advection of heat and water vapor into the South Pacific Ocean sector also corresponds with an increase in low cloud cover (shading; Figure 5), as well as an increase in cloud liquid water path (Figure 6) and atmospheric stability (Figure 9). In the winter, sea level pressure decreases in the Australian sector in both reanalyses (Figures 11a and 11b), which causes local anomalous cyclonic motion that advects colder and drier air off of Antarctica over the ocean (Figures 12a and 12b). Both water vapor and heat fluxes are very small here; the Australian sector also either shows reduced cloud cover (Figure 5a) or negligible cloud cover changes (Figure 5b).

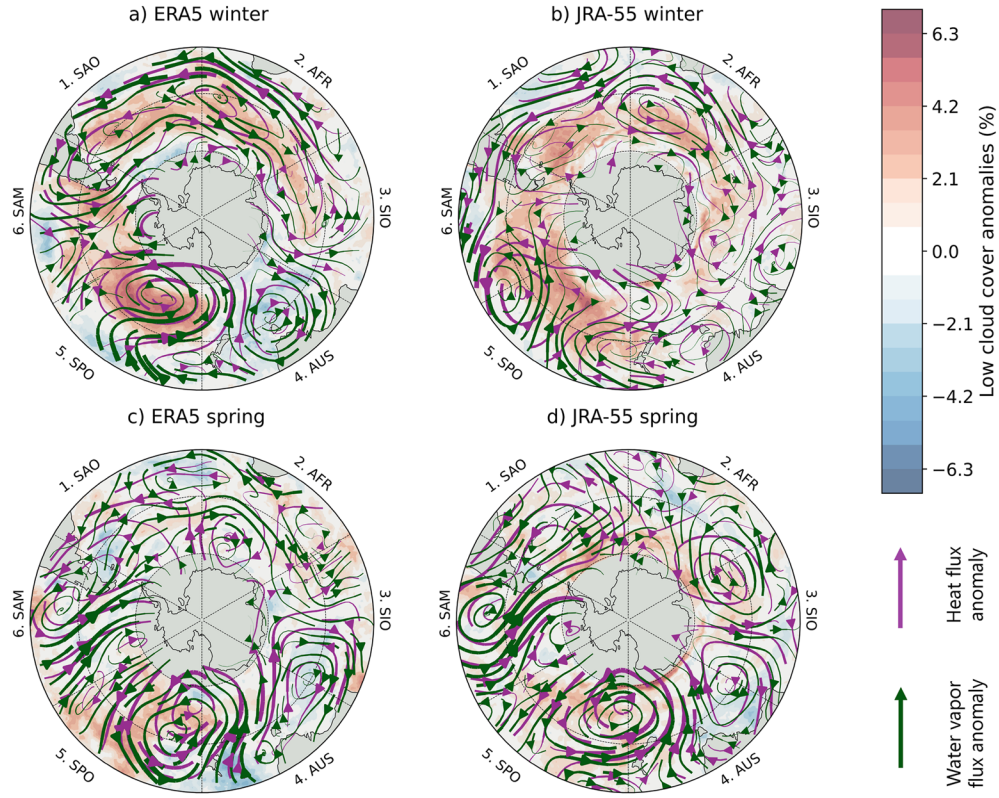

Figure 12. Regression of seasonal mean heat (purple) and water vapor (green) fluxes, shown as streamlines, on the seasonal Southern Ocean heat uptake index for (a) ERA5 winter, (b) JRA-55 winter, (c) ERA5 spring, and (d) JRA-55 spring. Streamline thickness is proportional to the magnitude of the normalized seasonal flux regression. Shading is the regression of seasonal low cloud cover on the seasonal Southern Ocean heat uptake index (Figure 5). The equatorward limit of Figure 12 is 30°S. The dotted lines at 45° and 65°S are the latitude limits of our defined Southern Ocean heat uptake index.

The advected heat and water vapor flux anomalies are generally larger in the spring (Figures 12c and 12d) than in the winter. In both reanalyses the largest fluxes are in the Australian, South Pacific Ocean, and South American sectors. As in the winter, advection of colder drier air off Antarctica reduces cloud cover between the South Indian Ocean and Australian sectors, which also corresponds to regions of reduced stability in ERA5 and JRA-55 (Figures 9c and 9d). As the atmosphere is already warmer in the spring than in winter, anomalous advection of heat and water vapor from lower latitudes likely has less impact on cloud cover in spring than in winter.

4. Discussion

One of the most important relationships shown in this study is the positive and significant ($p < 0.05$) relationship between winter cloud liquid water path and SOHU over the past 42 years, indicating that changes in clouds and their associated atmospheric states are linked to higher heat retention by the Southern Ocean during the coldest season. Increases in cloud liquid water path are more consequential for ocean heat uptake than just an increase in cloud cover. Why does the supercooled liquid water content of Southern Ocean clouds increase in the first place? The initial increase appears to be tied to large-scale synoptic processes that affect local environmental conditions. Southern Ocean clouds respond to changing environmental conditions (i.e., sea level pressure and water vapor/heat flux advection), and in turn appear to maintain environmental conditions favorable to increased SOHU. They participate in, but probably do not initiate, the chain reaction of events and interactions that affect SOHU. Anomalies in sea level pressure and corresponding changes in water vapor and temperature advection are likely related to large-scale phenomena like the Southern Annular Mode (SAM; Limpasuvan & Hartmann, 1999), which has regional impacts on temperature and storm tracks around the Southern Ocean (e.g., Gillett et al., 2006), or the Southern Oscillation Index (SOI; Trenberth, 1984). However, we find no significant correlation between either of the winter/spring SAM and SOI values (calculated using 1981–2010 as the normalizing base period) and the

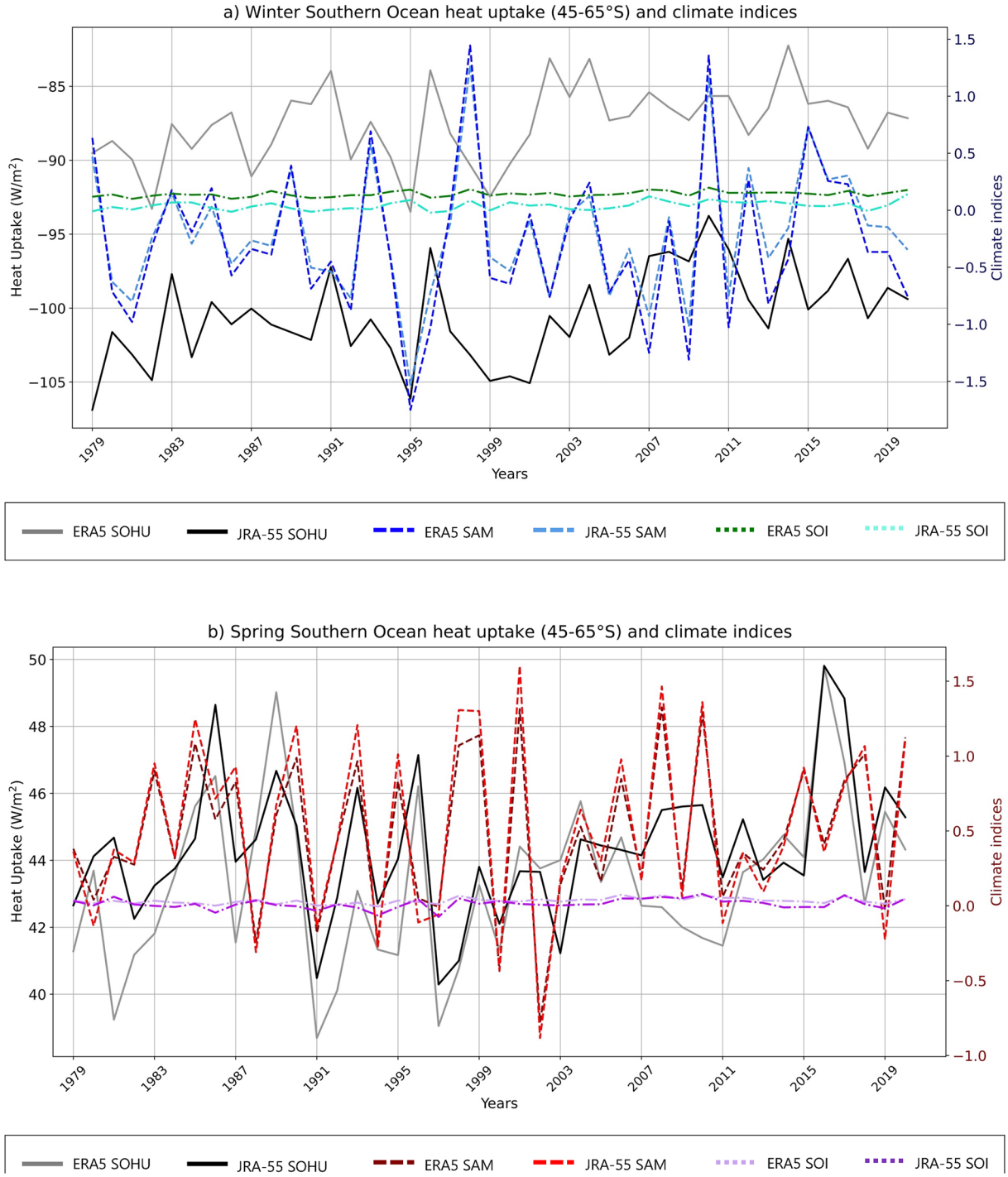

Figure 13. Time series of seasonal mean Southern Ocean heat uptake (45°–65°S; solid lines), Southern Annular Mode (SAM; dashed lines), and Southern Oscillation (SOI; dotted lines) indices from 1979 to 2020 for (a) winter and (b) spring in ERA5 and JRA-55. Note the scale differences for the winter and spring panels.

winter/spring SOHU indices in ERA5 and JRA-55 (Figure 13; correlation coefficient within 0.21 of zero; see Table S1 in Supporting Information S1 for the seasonal correlation coefficients). A complete diagnosis of the phenomena responsible for changing environmental conditions during high SOHU is outside the scope of this paper but will be a focus for future work.

In the meantime, many components of the interplay between clouds and ocean heat uptake are clear: warm air intrusions carrying heat and moisture toward the pole (e.g., Figure 12) provide a water vapor source for cloud formation, and can also change tropospheric stability, affecting cloud cover (e.g., Klein & Hartmann, 1993). Increased cloud cover, liquid water content, and water vapor will reduce surface longwave emission to space, but other factors are also important: the increased stability near the surface will directly suppress turbulent heat fluxes out of the ocean, and reduce heat loss to the atmosphere. These results show that ocean heat uptake is not a passive oceanic process, but that the atmosphere influences seasonal SOHU.

While many of the relationships described above are fairly robust during the winter, most relationships start to weaken during the spring. We believe there are three reasons for the weaker springtime relationships: (a) atmospheric energy transport into the Southern Ocean region is stronger during winter, (b) atmospheric states are more controlled by local processes during spring than during winter, and (c) springtime sea ice melt affects the Southern Ocean's ability to absorb heat from the atmosphere.

First, stronger poleward energy transport in the winter than during spring (Donohoe et al., 2013) affects seasonal mean air temperature and humidity. During the coldest season, heat and moisture advected over the Southern Ocean may have a larger effect on clouds than such advection during a warmer season. When the air-sea temperature gradient is large, as in winter, bringing warmer air from lower latitudes will increase the static stability faster than when the air-sea temperature gradient is smaller (Figure 9). Since the Southern Ocean atmosphere is often unstable (Bharti et al., 2019), small increases in atmospheric stability can have large impacts on turbulent heat fluxes out of the ocean. In the winter, SOHU increases from a combination of increased longwave fluxes caused by changes in clouds, air temperature, and humidity, and reduced turbulent heat fluxes out of the ocean caused by increased atmospheric stability. In the spring, positive SOHU anomalies are mainly driven by reduced turbulent heat fluxes caused by increased atmospheric stability. Over the entire Southern Ocean, the magnitude of winter and spring turbulent heat flux anomalies are similar for both reanalyses in winter and spring. Correlations between heat flux and heat uptake are also similar and significant: larger than -0.6 in both seasons and both reanalyses ($p < 0.05$).

Second, if spring atmospheric states are not strongly influenced by advection from lower latitudes, then they are controlled by more local processes. One such process, which affects cloud formation, is the availability of marine aerosols for cloud condensation nuclei (McCoy et al., 2015). Another process, which is a third reason why winter and spring atmosphere-SOHU relationships are different, is melting sea ice. Clouds preferentially form over newly open water during the spring (Frey et al., 2018), so clouds may be changing in response to melting sea ice instead of heat and moisture advection. Furthermore, sea ice melt during spring may reduce the Southern Ocean's ability to absorb heat from the atmosphere. Melting sea ice freshens the surface ocean layer, reducing density and increasing the stability of the ocean column, thereby inhibiting processes that transport surface heat to the deep Southern Ocean (Bitz et al., 2006; Gille et al., 2016; Gregory, 2000; Morrison et al., 2015). When more heat stays in the surface ocean, less heat is absorbed from the atmosphere into the ocean. Therefore, years with anomalously high sea ice extent may have anomalously high heat absorption from the atmosphere, leading to positive SOHU anomalies.

Even though relationships between SOHU and atmospheric properties weaken in the spring, SOHU anomalies are still larger than summer or fall anomalies. Since air temperature is warmest during summer, warm and wet air from lower latitudes advected over the Southern Ocean has the smallest effect on cloud cover, cloud liquid water path, and atmospheric stability compared to winter and spring. The temperature gradient between higher and lower Southern latitudes becomes stronger in the fall, but not as strong as in the winter and spring, which may be why the fall ocean heat uptake anomaly is stronger than the summer but weaker than the spring anomaly. The surface mixing inhibition caused by sea ice melt is also a phenomenon that occurs in the spring, not the fall, which is another reason why spring and fall SOHU anomalies may be different.

Given the impact that clouds have on winter SOHU, do we expect the magnitude or timing of SOHU to increase in a warming world? Satellite observations and climate models suggest a positive decadal trend in cloud liquid water path over the Southern Ocean (Manaster et al., 2017). If the observed cloud-SOHU relationship is solely due to a large-scale motion whose interannual variability remains the same, then we expect the SOHU to remain fairly constant. If, as is more likely, the cloud-SOHU relationship depends both on large-scale climate phenomena and the trend in cloud liquid water path, then we expect SOHU to increase at the same rate as cloud liquid water

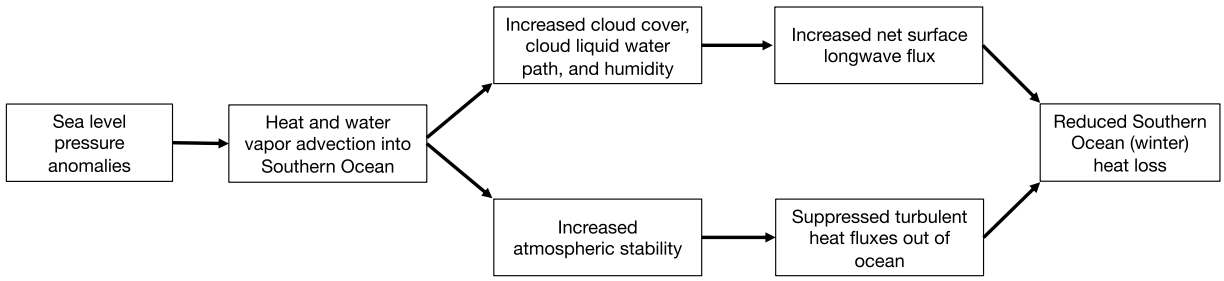

Figure 14. Schematic demonstrating how sea level pressure anomalies lead to atmospheric conditions that increase Southern Ocean heat uptake.

path. However, assessing future trends in cloud liquid water path are complicated by the fact that Southern Ocean clouds are not bright enough in the current generation of climate models.

The Southern Ocean is both poorly observed on a pan-regional, all-season scale and clouds are inadequately modeled, with known biases in supercooled liquid water amount (e.g., Bodas-Salcedo et al., 2014, 2016). Biases in cloud liquid water lead to biases in reflected shortwave and downwelling longwave radiation, both of which have significant implications for SOHU. As we have shown here, increased downwelling longwave radiation from cloud cover and liquid water is an important contributor to observed SOHU. If modeled clouds are not widespread enough, or do not contain enough supercooled liquid water, then SOHU is likely underestimated in climate models. Given the global importance of heat uptake and heat content around the Southern Ocean, an underestimation of SOHU has further knock-on effects for models' global climate. The results from this work may provide an observational constraint for atmospheric impacts on the mechanisms of ocean heat uptake.

5. Summary and Conclusions

In this study, we present the influence of clouds and other atmospheric processes on the mechanisms of SOHU in the ERA5 and JRA-55 reanalyses. By regressing seasonal anomalies on the SOHU index, we evaluate atmospheric states when SOHU is anomalously high compared to the 1979–2020 climatology and find:

- On average across the Southern Ocean, during the winter (spring) the Southern Ocean loses heat to (gains heat from) the atmosphere, but years with anomalously high SOHU are dominated by a decrease in heat loss to the atmosphere during winter and an increase in heat gain from the atmosphere during spring. Anomalously high SOHU is not controlled by an increase in ocean heat gain during summer.
- Increased cloud cover, liquid water path, and humidity cause stronger SOHU by increasing downwelling longwave radiation into the surface, but the effect is stronger in winter than in spring.
- Increased cloud cover is associated with a more stable lower atmosphere because the 800 mb air temperature is warmer than the surface during times of anomalously large cloud cover.
- Increased atmospheric stability suppresses turbulent heat fluxes out of the surface, keeping more heat in the ocean.
- Large-scale synoptic shifts in winter and spring sea level pressure and water vapor/heat flux advection are likely responsible for initiating the environmental changes around the Southern Ocean that correspond to changing atmospheric conditions that lead to an increase in cloud cover, cloud liquid water path, and atmospheric stability. These changes ultimately increase ocean heat uptake by reducing heat loss to the atmosphere (Figure 14).

While reanalyses are not true observations and results should be interpreted with some caution, these results provide a form of observational constraint on seasonal SOHU and the influence of clouds on SOHU from 1979 to 2020.

Conflict of Interest

The authors declare no conflicts of interest relevant to this study.

Data Availability Statement

All ERA5 data used for this study are publicly available from Copernicus Climate Change Service at https://cds.climate.copernicus.eu/cdsapp#!/home, and all JRA-55 data are publicly available from the Japan Meteorological Agency (JMA) and the National Center for Atmospheric Research (NCAR)'s Research Data Archive at https://rda.ucar.edu/datasets/ds628.1/.

Acknowledgments
Ariel L. Morrison and Philip J. Rasch were supported by the Regional and Global Model Analysis (RGMA) component of the Earth and Environmental System Modeling (EESM) program of the U.S. Department of Energy's Office of Science, as contribution to the HiLAT-RASM project. Ariel L. Morrison and Hansi A. Singh were supported by the University of Victoria. This research also used resources of the National Energy Research Scientific Computing (NERSC) Center, a DOE Office of Science User Facility supported by the Office of Science of the U.S. Department of Energy under Contract DE-AC02-05CH11231. The Pacific Northwest National Laboratory is operated for the U.S. Department of Energy by Battelle Memorial Institute under contract DE-AC05-76RL01830. The authors would like to thank R. Wood and three anonymous reviewers for helpful comments on this manuscript.

References

Armour, K. C., Marshall, J., Scott, J. R., Donohoe, A., & Newsom, E. R. (2016). Southern Ocean warming delayed by circumpolar upwelling and equatorward transport. *Nature Geoscience*, *9*, 549–554. https://doi.org/10.1038/ngeo2731

Bharti, V., Fairall, C., Blomquist, B., Huang, Y., Protat, A., Sullivan, P., et al. (2019). Air-sea heat and momentum fluxes in the Southern Ocean. *Journal of Geophysical Research: Atmospheres*, *124*(23), 12426–12443. https://doi.org/10.1029/2018JD029761

Bitz, C. M., Gent, P. R., Woodgate, R. A., Holland, M. M., & Lindsay, R. (2006). The influence of sea ice on ocean heat uptake in response to increasing CO_2. *Journal of Climate*, *19*, 2437–2450. https://doi.org/10.1175/jcli3756.1

Bodas-Salcedo, A., Hill, P. G., Furtado, K., Williams, K. D., Field, P. R., Manners, J. C., et al. (2016). Large contribution of supercooled liquid clouds to the solar radiation budget of the Southern Ocean. *Journal of Climate*, *29*(11), 4213–4228. https://doi.org/10.1175/jcli-d-15-0564.1

Bodas-Salcedo, A., Williams, K. D., Ringer, M. A., Beau, I., Cole, J. N. S., Dufresne, J.-L., et al. (2014). Origins of the solar radiation biases over the Southern Ocean in CFMIP2 models. *Journal of Climate*, *27*(1), 41–56. https://doi.org/10.1175/jcli-d-13-00169.1

Bourassa, M. A., Gille, S. T., Bitz, C., Carlson, D., Cerovecki, I., Clayson, C. A., et al. (2013). High-latitude ocean and sea ice surface fluxes: Challenges for climate research. *Bulletin of the American Meteorological Society*, *94*(3), 403–423. https://doi.org/10.1175/bams-d-11-00244.1

Deser, C., Hurrell, J. W., & Phillips, A. S. (2017). The role of the North Atlantic Oscillation in European climate projections. *Climate Dynamics*, *49*, 3141–3157. https://doi.org/10.1007/s00382-016-3502-z

Doddridge, E. W., Marshall, J., Song, H., Campin, J.-M., & Kelley, M. (2021). Southern Ocean heat storage, reemergence, and winter sea ice decline induced by summertime winds. *Journal of Climate*, *34*(4), 1403–1415. https://doi.org/10.1175/jcli-d-20-0322.1

Dong, S., Gille, S. T., & Sprintall, J. (2007). An assessment of the Southern Ocean mixed layer heat budget. *Journal of Climate*, *20*(17), 4425–4442. https://doi.org/10.1175/JCLI4259.1

Donohoe, A., Marshall, J., Ferreira, D., & Mcgee, D. (2013). The relationship between ITCZ location and cross-equatorial atmospheric heat transport: From the seasonal cycle to the last glacial maximum. *Journal of Climate*, *26*(11), 3597–3618. https://doi.org/10.1175/jcli-d-12-00467.1

Eyring, V., Bony, S., Meehl, G. A., Senior, C. A., Stevens, B., Stouffer, R. J., & Taylor, K. E. (2016). Overview of the coupled model intercomparison project phase 6 (CMIP6) experimental design and organization. *Geoscientific Model Development*, *9*, 1937–1958. https://doi.org/10.5194/gmd-9-1937-2016

Frey, W. R., Morrison, A. L., Kay, J. E., Guzman, R., & Chepfer, H. (2018). The combined influence of observed Southern Ocean clouds and sea ice on top-of-atmosphere albedo. *Journal of Geophysical Research: Atmospheres*, *123*, 4461–4475. https://doi.org/10.1029/2018jd028505

Frölicher, T. L., Sarmiento, J. L., Paynter, D. J., Dunne, J. P., Krasting, J. P., & Winton, M. (2015). Dominance of the Southern Ocean in anthropogenic carbon and heat uptake in CMIP5 models. *Journal of Climate*, *28*, 862–886.

Gille, S., Josey, S., & Swart, S. (2016). New approaches for air-sea fluxes in the Southern Ocean. *Eos*, *97*. https://doi.org/10.1029/2016EO052243

Gille, S. T. (2008). Decadal-scale temperature trends in the southern Hemisphere ocean. *Journal of Climate*, *21*(18), 4749–4765. https://doi.org/10.1175/2008JCLI2131.1

Gillett, N. P., Kell, T. D., & Jones, P. D. (2006). Regional climate impacts of the southern annular Mode. *Geophysical Research Letters*, *33*(23), L23704. https://doi.org/10.1029/2006gl027721

Gregory, J. (2000). Vertical heat transports in the ocean and their effect on time-dependent climate change. *Climate Dynamics*, *16*(7), 501–515. https://doi.org/10.1007/s003820000059

Haynes, J. M., Jakob, C., Rossow, W. B., Tselioudis, G., & Brown, J. (2011). Major characteristics of Southern Ocean cloud regimes and their effects on the energy budget. *Journal of Climate*, *24*(19), 5061–5080. https://doi.org/10.1175/2011jcli4052.1

Hersbach, H., Bell, B., Berrisford, P., Hirahara, S., Horányi, A., Muñoz-Sabater, J., et al. (2020). The ERA5 global reanalysis. *Quarterly Journal of the Royal Meteorological Society*, *146*(730), 1999–2049. https://doi.org/10.1002/qj.3803

Holte, J. W., Talley, L. D., Chereskin, T. K., & Sloyan, B. M. (2012). The role of air-sea fluxes in Subantarctic Mode Water formation. *Journal of Geophysical Research: Oceans*, *117*, C03040. https://doi.org/10.1029/2011jc007798

Huang, Y., Siems, S. T., Manton, M. J., Protat, A., & Delanoë, J. (2012). A study on the low-altitude clouds over the Southern Ocean using the DARDAR-MASK. *Journal of Geophysical Research: Atmospheres*, *117*, D18204. https://doi.org/10.1029/2012jd017800

Hyder, P., Edwards, J. M., Allan, R. P., Hewitt, H. T., Bracegirdle, T. J., Gregory, J. M., et al. (2018). Critical Southern Ocean climate model biases traced to atmospheric model cloud errors. *Nature Communications*, *9*(3625), 1–17. https://doi.org/10.1038/s41467-018-06662-8

Josey, S. A., Kent, E. C., & Taylor, P. K. (1999). New insights into the ocean heat budget closure problem from analysis of the SOC air-sea flux climatology. *Journal of Climate*, *12*(9), 2856–2880. https://doi.org/10.1175/1520-0442(1999)012<2856:niitoh>2.0.co;2

Kelleher, M. K., & Grise, K. M. (2019). Examining Southern Ocean cloud controlling factors on daily time scales and their connections to mid-latitude weather systems. *Journal of Climate*, *32*(16), 5145–5160. https://doi.org/10.1175/jcli-d-18-0840.1

Klein, S. A., & Hartmann, D. (1993). The seasonal cycle of low stratiform clouds. *Journal of Climate*, *6*(8), 1587–1606. https://doi.org/10.1175/1520-0442(1993)006<1587:tscols>2.0.co;2

Kobayashi, S., Ota, Y., Harada, Y., Ebita, A., Moriya, M., Onoda, H., et al. (2015). The JRA-55 reanalysis: General specifications and basic characteristics. *Journal of the Meteorological Society of Japan*, *93*(1), 5–48. https://doi.org/10.2151/jmsj.2015-001

Lawson, R. P., & Gettelman, A. (2014). Impact of Antarctic mixed-phase clouds on climate. *Proceedings of the National Academy of Sciences*, *111*(51), 18156–18161. https://doi.org/10.1073/pnas.1418197111

Limpasuvan, V., & Hartmann, D. L. (1999). Eddies and the annular modes of climate variability. *Geophysical Research Letters*, *26*(20), 3133–3136. https://doi.org/10.1029/1999gl010478

Liu, J., Xiao, T., & Chen, L. (2011). Intercomparisons of air-sea heat fluxes over the Southern Ocean. *Journal of Climate*, *24*(4), 1198–1211. https://doi.org/10.1175/2010jcli3699.1

Llovel, W., & Terray, L. (2016). Observed southern upper-ocean warming over 2005-2014 and associated mechanisms. *Environmental Research Letters*, *11*, 124023. https://doi.org/10.1088/1748-9326/11/12/124023

Mace, G. G., Protat, A., Humphries, R. S., Alexander, S. P., McRobert, I. M., Ward, J., et al. (2020). Southern Ocean cloud properties derived from CAPRICORN and MARCUS data. *Journal of Geophysical Research: Atmospheres*, *126*, e2020JD033368. https://doi.org/10.1029/2020JD033368

Mace, G. G., & Zhang, Q. (2014). The CloudSat radar-lidar geometrical profile product (RL-GeoProf): Updates, improvements, and selected results. *Journal of Geophysical Research: Atmospheres*, *119*, 9441–9462. https://doi.org/10.1002/2013jd021374

Manaster, A., O'Dell, C. W., & Elsaesser, G. (2017). Evaluation of cloud liquid water path trends using a multidecadal record of passive microwave observations. *Journal of Climate*, *30*, 5871–5884. https://doi.org/10.1175/jcli-d-16-0399.1

McCoy, D. T., BurrowsWood, S. M. R., Grosvenor, D. P., Elliot, S. M., Ma, P.-L., Rasch, P. J., et al. (2015). Natural aerosols explain seasonal and spatial patterns of Southern Ocean cloud albedo. *Science Advances*, *1*(6), 1–12. https://doi.org/10.1126/sciadv.1500157

Mo, K. C., & White, G. H. (1985). Teleconnections in the southern Hemisphere. *Monthly Weather Review*, *113*, 22–37. https://doi.org/10.1175/1520-0493(1985)113<0022:titsh>2.0.co;2

Morrison, A. K., Frölicher, T. L., & Sarmiento, J. L. (2015). Upwelling in the Southern Ocean. *Physics Today*, *68*, 27–32. https://doi.org/10.1063/pt.3.2654

Morrison, A. K., Griffies, S. M., Winton, M., Anderson, W. G., & Sarmiento, J. L. (2016). Mechanisms of Southern Ocean heat uptake and transport in a global eddying climate model. *Journal of Climate*, *29*(6), 2059–2075. https://doi.org/10.1175/jcli-d-15-0579.1

Naud, C. M., Booth, J. F., & Del Genio, A. D. (2014). Evaluation of ERA-interim and MERRA cloudiness in the Southern Ocean. *Journal of Climate*, *27*(5), 2109–2124. https://doi.org/10.1175/jcli-d-13-00432.1

Naud, C. M., Booth, J. F., Lamer, K., Marchand, R., Protat, A., & McFarquhar, G. M. (2020). On the relationship between the marine cold air outbreak M parameter and low-level cloud heights in the midlatitudes. *Journal of Geophysical Research: Atmospheres*, *125*, e2020JD032465. https://doi.org/10.1029/2020JD032465

Newsom, E. R., Bitz, C. M., Bryan, F. O., Abernathey, R., & Gent, P. R. (2016). Southern Ocean deep circulation and heat uptake in a high-resolution climate model. *Journal of Climate*, *29*(7), 2597–2619. https://doi.org/10.1175/jcli-d-15-0513.1

Ogle, S. E., Tamsitt, V., Josey, S. A., Gille, S. T., Cerovečki, I., Talley, L. D., & Weller, R. A. (2018). Episodic Southern Ocean heat loss and its mixed layer impacts revealed by the farthest south multiyear surface flux mooring. *Geophysical Research Letters*, *45*(10), 5002–5010. https://doi.org/10.1029/2017GL076909

Purkey, S. G., & Johnson, G. C. (2010). Warming of global Abyssal and deep Southern Ocean waters between the 1990s and 2000s: Contributions to global heat and sea level rise budgets. *Journal of Climate*, *23*(23), 6336–6351. https://doi.org/10.1175/2010jcli3682.1

Rafael, M. N. (2004). A zonal wave 3 index for the Southern Hemisphere. *Geophysical Research Letters*, *31*(23), 1–4. https://doi.org/10.1029/2004GL020365

Rhein, M., Rintoul, S. R., Aoki, S., Campos, E., Chambers, D., Feely, R. A., et al. (2013). Observations: Ocean. In T. F. Stocker, D. Qin, G.-K. Plattner, M. Tignor, S. K. Allen, J. Boschung, A. Nauels, Y. Xia, V. Bex, & P. M. Midgley (Eds.), *Climate change 2013: The physical science basis. Contribution of working Group I to the Fifth Assessment report of the Intergovernmental panel on climate change* (p. 255–315). Cambridge University Press.

Rose, B. E. J., & Rayborn, L. (2016). The effects of ocean heat uptake on transient climate sensitivity. *Current Climate Change Reports*, *2*, 190–201. https://doi.org/10.1007/s40641-016-0048-4

Sallé, J.-B. (2018). Southern Ocean warming. *Oceanography*, *31*(2), 52–62. https://doi.org/10.5670/oceanog.2018.215

Shi, J.-R., Xie, S.-P., & Talley, L. D. (2018). Evolving relative importance of the Southern Ocean and north Atlantic in anthropogenic ocean heat uptake. *Journal of Climate*, *31*(18), 7459–7479. https://doi.org/10.1175/jcli-d-18-0170.1

Shupe, M. D., & Intrieri, J. M. (2004). Cloud radiative forcing of the Arctic surface: The influence of cloud properties, surface albedo, and solar zenith angle. *Journal of Climate*, *17*(3), 616–628. https://doi.org/10.1175/1520-0442(2004)017<0616:crfota>2.0.co;2

Swart, S., Gille, S. T., Delille, B., Josey, S., Mazloff, M., Newman, L., et al. (2019). Constraining Southern Ocean air-sea-ice fluxes through enhanced observations. *Frontiers in Marine Science*, *6*, 421. https://doi.org/10.3389/fmars.2019.00421

Taylor, K. E., Stouffer, R. J., & Meehl, G. A. (2012). An overview of CMIP5 and the experiment design. *Bulletin of the American Meteorological Society*, *93*(4), 485–498. https://doi.org/10.1175/bams-d-11-00094.1

Trenberth, K. (1984). Signal versus noise in the southern oscillation. *Monthly Weather Review*, *112*, 326–332. https://doi.org/10.1175/1520-0493(1984)112<0326:svnits>2.0.co;2

Trossman, D. S., Palter, J. B., Merlis, T. M., Huang, Y., & Xia, Y. (2016). Large-scale ocean circulation-cloud interactions reduce the pace of transient climate change. *Geophysical Research Letters*, *43*(8), 3935–3943. https://doi.org/10.1002/2016GL067931

Tsujino, H., Urakawa, S., Nakano, H., Small, R. J., Kim, W. M., Yeager, S. G., et al. (2018). JRA-55 surface based dataset for driving ocean-sea-ice models (JRA55-do). *Ocean Modelling*, *130*, 79–139. https://doi.org/10.1016/j.ocemod.2018.07.002

Vergara-Temprado, J., Miltenberger, A. K., Furtado, K., Grosvenor, D. P., Shipway, B. J., Hill, A. A., et al. (2018). Strong control of Southern Ocean cloud reflectivity by ice-nucleating particles. *Proceedings of the National Academy of Sciences*, *115*(11), 2687–2692. https://doi.org/10.1073/pnas.1721627115

Wang, H., Klekociuk, A. R., French, W. J. R., Alexander, S. P., & Warner, T. A. (2020). Measurements of cloud radiative effect across the Southern Ocean (43° S-79° S, 63° E-158° W). *Atmosphere*, *11*(949), 1–22. https://doi.org/10.3390/atmos11090949

Warren, S. G., Hahn, C. H., London, J., Chervin, R. M., & Jenne, R. L. (1988), *Global distribution of total cloud cover and cloud type amounts over the ocean, (No. DOE/ER-0406; NCAR/TN--317-STR)*. USDOE Office of Energy Research, Washington, DC (USA). Carbon Dioxide Research Div.; Natl. Cent. for Atmos. Res., Boulder, Colo. https://doi.org/10.5065/D6QC01D1

Wood, R., & Bretherton, C. S. (2006). On the relationship between stratiform low cloud cover and lower-tropospheric stability. *Journal of Climate*, *19*(24), 6425–6432. https://doi.org/10.1175/jcli3988.1